

Quantum State Tomography of BECs and Atom Lasers

Andrew James Ferris



A thesis submitted for the degree of
Bachelor of Science with Honours in Theoretical Physics
of The Australian National University

October, 2004

Declaration

This thesis is an account of research undertaken under the supervision of Dr Joseph Hope between February 2004 and October 2004 at the Australian Research Council's Center of Excellence for Quantum-Atom Optics, The Department of Physics, Faculty of Science, The Australian National University, Canberra, Australia.

Except where acknowledged in the customary manner, the material presented in this thesis is, to the best of my knowledge, original and has not been submitted in whole or part for a degree in any university.

Andrew James Ferris
October, 2004

Acknowledgements

There are many people that I would like to thank. Here are the ones I can remember.

Most of all, I would like to thank my supervisor, Dr Joseph Hope. I have thoroughly appreciated Joe's supervision and guidance over the years. Joe took the time to educate me in the ways of BEC when I was a mere second year student. Practically all of my knowledge of atom optics and field theory are due to him. Thanks Joe!

I would also like to thank Simon Haine, for always being there to ask questions, argue with, play guitar, annoy; and for his bouncy ball seat.

Thank you to Dr Craig Savage, for being available to give me advice and for interesting discussions on quantum mechanics. I would also like to thank Craig for the many inspiration lectures on quantum mechanics that I have received, and for being a caring honours co-ordinator.

Thanks also to my other office mates. Adele Morrison has been a great friend ever since my first 'real' contact with physics. I would like to thank Tom Hanna for his research and interesting discussions on phase, measurement and atoms. Thanks John Close for random discussions and distraction. And thank you to all the other members of the group, for making such a great environment to work in.

I thank Dr Pin Koy Lam, Prof. Hans Bachor, Magnus Hsu and the rest of quantum optics group, for answering all my questions on squeezing.

Thanks to Patrick Scott, for an interesting, drunken (and yet useful) conversation on the measurement of phase.

I would like to Tim Burgess for some advice on \LaTeX , for his \LaTeX book. Thanks Tim and Luke for offering me a room.

Thanks to all the honours kiddies for helping make this such a good year. Thanks to everyone I've enjoyed a drink with, and thanks to the inventor of home-brew.

Thanks Sarah, for being supportive throughout the year. I'm sure I would have gone crazy without you. Thank you to all my housemates: Sar, TIMMAH!, DJ Shortcake, Patty-B, Luke, Max, Benji, and Ducky. Thanks Jess for being a whinger.

Abstract

The quantum state of a dilute-gas Bose-Einstein condensate (BEC) was of interest even before BEC was experimentally achieved. We would like to be able to determine the state of a BEC experimentally, by performing a quantum state reconstruction experiment on a BEC. In this thesis we analyse precisely what is able to be measured in a system of ultra-cold bosonic atoms. We suggest some techniques for performing quantum state tomography that can be applied to atom lasers.

Due to the existence of super-selection rules of the Hamiltonian (which acts to conserve the number of atoms), it is shown that every observable that can be measured for conserved particles must be quadratic¹ in form. If we begin with a field of thermal bosonic atoms, then no matter how they evolve, no ‘absolute phase information’ is measurable about any mode of these atoms. Only statistics relating to the number of particles can be measured for a single mode dilute-gas BEC.

However, this does not rule out the possibility of correlations between different modes, leading to ‘relative phase information’. It is shown that the quantum state representing these correlations can be reconstructed by adapting a tomographic technique used in quantum-optics known as self-homodyne tomography. We analyse the effectiveness of such a technique in the regime of low atom numbers.

When performing a tomography experiment, it is necessary to rotate the quadrature angle. We propose several methods of achieving quadrature rotation in a system containing an atom laser with side-band correlations. In particular, due to the fact that atoms disperse in free space, we can rotate the quadrature angle simply by allowing the atom laser to travel. The experimenter could also use controlled potentials to rotate quadrature. Finally, the gravitational potential is considered.

¹Quadratic operators contain equal numbers of annihilation and creation operators in each term. e.g. $\hat{a}^\dagger\hat{a}$ is quadratic, but $\hat{a} + \hat{a}^\dagger$ is not.

Contents

Declaration	i
Acknowledgements	iii
Abstract	v
1 Introduction	1
2 Background Theory	5
2.1 Introduction to Quantum Field Theory	5
2.1.1 Density Matrices	7
2.1.2 Common Photon Fields	9
2.1.3 Operator Ordering	11
2.2 Phase-Space Diagrams of Quantum States	11
2.2.1 Q , P and Wigner Functions	12
2.2.2 The s -parameterised QPD	21
3 Literature Review	23
3.1 Quantum State Tomography	23
3.1.1 Single-Particle State Tomography	23
3.1.2 The Inverse-Radon Transformation	24
3.1.3 Other Reconstruction Methods	25
3.2 Quantum Optics	25
3.2.1 Direct Detection	25
3.2.2 Standard Homodyne Detection	26
3.2.3 Optical Homodyne Tomography	28
3.2.4 Self-Homodyne Tomography	29
3.3 The State of BEC	32
3.3.1 Theoretical Progress	32
3.3.2 Experimental Results	34
3.3.3 Perturbed BEC	34
3.4 Absolute and Relative Phase References	35
4 Detection of BEC	37
4.1 Single-Mode Detection	37
4.1.1 Single-Mode Closed Systems	37
4.1.2 Measuring with Vacuum?	38
4.1.3 An Infinite Amount of Nothing	43
4.1.4 The Requirements of Measurement	45
4.2 Single Trap BEC	46
4.2.1 Unstable Bosons	46
4.2.2 Measurement of Trapped Dilute-Gas BEC	47

4.2.3	In Hindsight...	49
5	Self-Homodyne Tomography for Atom Lasers	51
5.1	Relative Phase References	51
5.2	Side-band Measurement	52
5.3	Limitations Due to Low Atom Numbers	53
5.4	Summary	56
6	Proposed Self-Homodyne Techniques For Atom Lasers	57
6.1	Dispersion in Free Space	57
6.1.1	Photons	58
6.1.2	Non-Relativistic Atoms	58
6.1.3	Numerical Substitution	59
6.2	Using Potential to Control Quadrature Angle	61
6.2.1	Simple Potential	62
6.2.2	General Potentials	64
6.3	Gravity	65
6.3.1	Vertical Motion	65
6.3.2	Two-Dimensional Motion	68
7	Conclusions	69
	Bibliography	71

Introduction

It is the nature of a physicist to try to understand everything in our universe. We typically look at a subsystem of the universe and attempt to break it down into smaller and smaller interacting systems. Once we understand the smaller systems, we can eventually build up the larger and more complicated systems we observe around us. This thesis aims to find methods to measure the ultimate detail of ultra-cold atomic sources - that is, their quantum state.

Bose-Einstein condensation (BEC) is a quantum phenomenon which was proposed theoretically in 1924 by the combined works of Bose and Einstein [1, 2]. Einstein had concluded that bosons (particles with integral spin) were able to *condense* into the same quantum state at extremely low temperature. For instance, bosonic Helium-4 becomes superfluid below just a few Kelvin. In 1938 Fritz-London hypothesised that superfluidity was related to Bose-Einstein condensation [3], and current models back up his claim. Part of the liquid Helium becomes a BEC and interacts in a seemingly co-operative way which explains the remarkable properties of a superfluid. Another example is a dilute gas BEC, first experimentally realised in 1995 with rubidium atoms [4]. Since then many BECs made of different species (such as sodium [5] and lithium [6]) have been made in laboratories around the world.

Of particular interest is the creation of metastable $^4\text{He}^*$ BEC, first achieved in 2001 [7, 8]. Helium has a metastable state (labelled 2^3S_1) with 19.82 eV of internal energy and lifetime 7900 seconds [9]. The long lifetime allows it to be used in experiments that run for many seconds. The energy from the metastable state can be released upon collision with another object. The energy is large enough to be picked up upon collision with a suitable detector. Such detectors are capable of measuring single atoms with a quantum efficiency of ~ 0.6 [47]. Single particle detection will be essential for measuring the precise quantum state of a BEC.

It is relatively recently that we saw the experimental realisation of dilute-gas Bose-Einstein condensates, and from these the first attempts at creating atom lasers have been made. Both of these objects are essentially a bosonic field of very cold atoms which are all approximately occupying the same quantum mode. BECs are most often modelled in a semi-classical mean-field approximation. This approach has, for the most part, been completely successful. This approximation makes assumptions regarding the number-statistics of the field (such as assuming they are in a coherent state). However, the validity of this assumption has not been well tested. To date, no one actually knows the quantum state of the BECs and atom lasers we create, and thus we can not claim to have full understanding of these objects.

For a perfect, zero temperature BEC, each particle is said to be in the same quantum state. This is the same as saying that it can be represented by a single mode bosonic field.

The only degree of freedom left in this field is the quantum statistics of the mode. For instance, in a single mode laser there is a purely quantum uncertainty in the number of photons in the laser beam. If we attempt to load atoms into a trap, each atom will end up in a quantum superposition of either in or out of the trap, and thus the state of the BEC field may be a superposition of many possible numbers of particles in the trap. Of course, it may be possible that there is a defined number of atoms in the trap. For example this could happen after making a measurement on total particle number where the state would be projected into the measured Fock state.

We can represent quantum states in many different ways. One popular method is to use quasi-probability distributions such as the Wigner function. The Wigner function is plotted against the conjugate variables of phase-space. For single mode fields these are called *quadratures* and are represented by a sum of the field operators (e.g. $\hat{a} + \hat{a}^\dagger$). The values of the Wigner function for some states will approximately represent the probability density of finding the state at a given point in phase-space - thus it is called a quasi-probability distribution. The Wigner function has some useful properties - it is real, bounded, continuous, normalised, and an exact representation of the density matrix for a system. The projection (column integration) of the Wigner function onto an axis will give the probability distribution for the observable that the axis represents.

Bertrand and Bertrand first suggested that tomographic methods could be used to reconstruct Wigner functions in quantum mechanics [10]. Tomography is the method of creating higher dimensional information from marginals (or projections) and is a technique used in technology such as the medical CAT scan. Vogel and Risken extended this idea [11], by suggesting a way of reconstructing a particular set of quasi-probability distribution functions from quadrature measurement distributions.

This method has been carried out frequently in the area of quantum optics to reconstruct the quantum state of several sources of light. This was first achieved by Smithey *et al.* [18, 19, 20] with a technique they called *optical homodyne tomography* (OHT). This technique relies on the existence of a ‘local oscillator’ which plays the role of a fixed phase reference. The local oscillator is typically a large coherent state laser beam. Similar methods have been applied to find the position/momentum Wigner function for an ensemble of helium atoms by Kurtsiefer *et al.* [21].

A way of performing homodyne tomography without a spatially separate local oscillator has been achieved [22, 23, 24] and is known as *self-homodyne tomography*. It relies on interference between different modes of a multi-mode field. The field must be in a ‘nearly’ coherent state for this technique to work. This is so that it can become its own phase reference in the homodyne measurement. However, this measurement scheme is limited to measuring quantum correlations between the different modes of the field, such as side-band correlations that can be created in lasers, and more recently shown to be transferable to atom-lasers [25].

We have not yet achieved a large, coherent source of atoms to be a local oscillator in an analogous experiment in atom optics. Thus OHT techniques can not be used to measure the quantum state of a BEC or an atom laser. Currently, the best method for measuring correlations between modes would be an analogous experiment to self-homodyne tomography.

The aim of this thesis is to find methods of quantum state tomography that can be applied in general to dilute-gas BECs and atom lasers (in particular, those made with $^4\text{He}^*$) with current resources. The ability to perform tomography on a single-mode field, such as a BEC, shall be investigated. The technique of self-homodyne tomography shall

be adapted for use with atoms. The experimental realisability, accuracy and reliability of such a method will be analysed.

Overview of this Thesis

We commence in chapter 2 with a presentation of some basic background material essential to this thesis. In this chapter, second quantisation is quickly introduced, along with some other basic quantum mechanical concepts such as density matrices. Phase-space diagrams are discussed and several quasi-probability distributions are defined and explained.

Chapter 3 constitutes a literature review of various topics applicable to this thesis. The principles of quantum state tomography are introduced, and methods of performing tomography experiments in quantum optics are discussed. Previous work looking at phase information in BEC is reviewed. Finally, an idea known as super-selection and its implication on phase references is discussed.

The results of this thesis are contained in chapters 4, 5 and 6. Chapter 4 deals primarily with the measurement of single mode bosonic fields, and the implications of this on BEC. In chapter 5, it is shown that a quantum-optics technique known as self-homodyne tomography can also be applied to atoms. Several experimental proposals to achieve this are discussed in chapter 6, and their practicality is discussed.

Finally, chapter 7 concludes this thesis, summing up the results and proposing directions for future work.

Background Theory

In this chapter we introduce some basic background material necessary throughout this thesis. The first section introduces second quantisation and some basic facts and definitions useful in field theory. The second section deals with the representation of quantum states using various quasi-probability distributions.

2.1 Introduction to Quantum Field Theory

The process of turning a classical Hamiltonian for a particle into a quantum Hamiltonian to describe the motion of the particle is called first quantisation. First quantisation deals adequately with one particle at a time. Second quantisation is the next step that creates quantum field theory. It involves quantising the field, that is quantising the number of particles in a state (or mode). In order to achieve this we introduce field operators for each mode of the particle type in question. For a discrete basis, for the k th mode, we denote the annihilation and creation operators as \hat{a}_k and \hat{a}_k^\dagger respectively. They follow commutation relations, depending on whether the quantum particle is a boson or a fermion:

$$\left[\hat{a}_j, \hat{a}_k^\dagger \right] = \delta_{jk} ; \quad \left[\hat{a}_j, \hat{a}_k \right] = \left[\hat{a}_j^\dagger, \hat{a}_k^\dagger \right] = 0, \quad (\text{bosons}) \quad (2.1a)$$

$$\left\{ \hat{a}_j, \hat{a}_k^\dagger \right\} = \delta_{jk} ; \quad \left\{ \hat{a}_j, \hat{a}_k \right\} = \left\{ \hat{a}_j^\dagger, \hat{a}_k^\dagger \right\} = 0. \quad (\text{fermions}) \quad (2.1b)$$

Take for example photons in a cavity. The cavity will only have certain resonant frequencies, ω_k , corresponding to a spatial mode $\mathbf{u}_k(\mathbf{r})$, which together represent the mode of a photon. We can always find a vector-potential $\mathbf{A}(\mathbf{r}, t)$ such that we can find the electric and magnetic fields $\mathbf{E}(\mathbf{r}, t)$ and $\mathbf{B}(\mathbf{r}, t)$ and expand in terms of the modes of the field:

$$\mathbf{E} = \frac{\partial \mathbf{A}}{\partial t}, \quad (2.2a)$$

$$\mathbf{B} = \nabla \times \mathbf{A}, \quad (2.2b)$$

$$\mathbf{A} = \sum_k \sqrt{\frac{\hbar}{2\omega_k \epsilon_0}} (a_k \mathbf{u}_k(\mathbf{r}) e^{-i\omega_k t} + a_k^* \mathbf{u}_k^*(\mathbf{r}) e^{i\omega_k t}). \quad (2.2c)$$

We know that the Hamiltonian (energy) of the system is given by:

$$H = \frac{1}{2} \int (\epsilon_0 \mathbf{E}^2 + \mu_0 \mathbf{H}^2) d^3 \mathbf{r}. \quad (2.3)$$

Now we note the similarities of this system with a harmonic oscillator. The two canonically conjugate variables are E and B . Every harmonic oscillator has the same ‘ladder’

style solution in quantum mechanics. If we compare the situation to the quantum harmonic oscillator, then the terms a_k and a_k^* are in the place of the ‘ladder operators’. If we wish to quantise the modes of the electromagnetic field (i.e. quantise the number of photons) than this would be achieved by placing the quantum ladder operators - which are always defined by the bosonic field operators. Second quantisation of the electromagnetic field is achieved by replacing a_k and a_k^* by the field operators \hat{a}_k and \hat{a}_k^\dagger . These are the bosonic field operators for the photons in mode k . The quantum Hamiltonian for the system can be determined by the classical energy, which can be found to be:

$$\hat{H} = \sum_k \hbar\omega_k \left(\hat{a}_k^\dagger \hat{a}_k + \frac{1}{2} \right). \quad (2.4)$$

It should be noted that when the modes are dependent on a continuous variable (position x , say), it is normal to use $\hat{\psi}(x)$ and $\hat{\psi}^\dagger(x)$ as the annihilation and creation operators.

Fock States

Now we have two operators for a mode, and we assume \hat{a} is an annihilation operator and \hat{a}^\dagger is a creation operator. We define the vacuum state $|0\rangle$ as the state from which it is impossible to annihilate a particle:

$$\hat{a}|0\rangle = 0. \quad (2.5)$$

The vacuum state can be seen as the state with no particles in it. We also define a Fock state $|n\rangle$, to be an eigenstate of the number operator $\hat{N} = \hat{a}^\dagger \hat{a}$:

$$\hat{N}|n\rangle = \hat{a}^\dagger \hat{a}|n\rangle = n|n\rangle. \quad (2.6)$$

This Fock state can be seen as the state with n particles in it. Since $\hat{a}^\dagger \hat{a}$ is the number operator, we can see that the energy of an electromagnetic field in a cavity from the Hamiltonian in equation 2.4 is

$$\bar{E} = \langle \hat{H} \rangle = \sum_k \hbar\omega \left(\bar{n}_k + \frac{1}{2} \right), \quad (2.7)$$

where \bar{n}_k is the expectation value of the number of particles (photons) in each mode. We can see how the annihilation and creation operators must work on Fock states, and we can thus write any Fock state in terms of the creation operator acting on the vacuum state:

$$\hat{a}|n\rangle = \sqrt{n}|n-1\rangle, \quad (2.8a)$$

$$\hat{a}^\dagger|n\rangle = \sqrt{n+1}|n+1\rangle, \quad (2.8b)$$

$$\therefore |n\rangle = \frac{(\hat{a}^\dagger)^n}{\sqrt{n!}}|0\rangle. \quad (2.8c)$$

It doesn't take much to show that the Fock states are orthogonal and that they are complete:

$$\langle n|m\rangle = \delta_{nm}, \quad (2.9a)$$

$$\sum_{n=0}^{\infty} |n\rangle\langle n| = \hat{1}. \quad (2.9b)$$

Thus the Fock states form a Hilbert space. They are a complete quantum description of the mode they represent, so we can write out any state of the field $|\psi\rangle$ in terms from this basis, with complex coefficients $c_n = \langle n|\psi\rangle$:

$$|\psi\rangle = \sum_n^{\infty} c_n |n\rangle. \quad (2.10)$$

With the machinery so far we could possibly solve a closed system with a known Hamiltonian. However, it is not very common that a system is in a Fock state, and it will pay to investigate some other common forms in which a state may be.

2.1.1 Density Matrices

Density Matrices for Pure States

Density matrices are an extremely useful way of formulating quantum mechanics. Not only do they deal properly with the quantum statistics of states, they can also take into account classical statistics due to classical uncertainties in the initial conditions of the system.

We define a pure state to be an ordinary quantum state that we can write as $|\psi\rangle$. For illustration, let this represent the state which has only two basis vectors, such as the spin of an electron being spin up or spin down. Then we can write $|\psi\rangle = c_1|\uparrow\rangle + c_2|\downarrow\rangle$, where c_1 and c_2 are two complex numbers and $|c_1|^2 + |c_2|^2 = 1$. This can be represented also in vector form:

$$\psi = \begin{bmatrix} c_1 \\ c_2 \end{bmatrix} = \begin{bmatrix} |c_1|e^{i\gamma_1} \\ |c_2|e^{i\gamma_2} \end{bmatrix}. \quad (2.11)$$

We can only experimentally measure the relative probabilities $\frac{|c_1|^2}{|c_2|^2}$ and the relative phase $\gamma_1 - \gamma_2$. We can write down ψ in terms of a density matrix ρ without losing any information:

$$\rho = \psi\psi^\dagger = \begin{bmatrix} c_1 \\ c_2 \end{bmatrix} \begin{bmatrix} c_1^* & c_2^* \end{bmatrix} = \begin{bmatrix} |c_1|^2 & c_1c_2^* \\ c_1^*c_2 & |c_2|^2 \end{bmatrix} = \begin{bmatrix} |c_1|^2 & |c_1c_2|e^{i(\gamma_1-\gamma_2)} \\ |c_1c_2|e^{i(\gamma_2-\gamma_1)} & |c_2|^2 \end{bmatrix}. \quad (2.12)$$

Notice that in this representation if we add an arbitrary phase into ψ we do not change the density matrix. The density matrix is Hermitian, and we note $\text{trace } \rho = 1$, where the trace of a matrix is the sum of its diagonal terms. This formulation of the density matrix extends to states represented by any complete, orthogonal vector basis (say $\{|i\rangle\}_i$), so in general the density matrix for the state ψ in vector form is:

$$\rho = \psi\psi^\dagger. \quad (2.13)$$

The same properties hold, ρ is Hermitian, its trace is always unity and the total phase of the original vector does not matter. The question is now, how do we get anything useful out of the density matrix? The expectation value for any operator \hat{A} can be found. We first write the operator in matrix form, then perform matrix multiplication and calculate

the trace:

$$A_{ij} = \langle i|\hat{A}|j\rangle, \quad (2.14a)$$

$$\begin{aligned} \langle \psi|\hat{A}|\psi\rangle &= \text{trace}[\rho\mathbf{A}] \\ &= \text{trace}[\mathbf{A}\rho]. \end{aligned} \quad (2.14b)$$

We can create the density operator from the bra-ket notation. Analogous to equation 2.13, we define:

$$\hat{\rho} = |\psi\rangle\langle\psi|. \quad (2.15)$$

The density operator can be simply expressed in terms of the density matrix:

$$\hat{\rho} = \sum_{i,j} \rho_{ij} |i\rangle\langle j|. \quad (2.16)$$

We define the trace of such an operator as:

$$\text{trace } \hat{\rho} = \sum_i \langle i|\hat{\rho}|i\rangle. \quad (2.17)$$

The density operator has the same properties as the density matrix - it is Hermitian and its trace is always unity. Again we can find the expectation value of an operator \hat{A} , analogous to equation 2.14b:

$$\langle \hat{A} \rangle = \text{trace}[\hat{\rho}\hat{A}] = \text{trace}[\hat{A}\hat{\rho}]. \quad (2.18)$$

In particular we can find the projection operator for any state $|\phi\rangle$ that tells us the probability of, upon measurement, finding the particle in state $|\phi\rangle$:

$$P(\phi) = |\langle\phi|\psi\rangle|^2 = \text{trace}[\hat{\rho}|\phi\rangle\langle\phi|]. \quad (2.19)$$

The next question is how does the density operator evolve? If in the Schrödinger picture we have

$$i\hbar \frac{\partial|\psi\rangle}{\partial t} = \hat{H}|\psi\rangle, \quad (2.20)$$

then we can obtain a Heisenberg equation of motion for the density operator:

$$i\hbar \frac{\partial\hat{\rho}}{\partial t} = [\hat{H}, \hat{\rho}]. \quad (2.21)$$

Density Matrices for Mixed States

This section introduces the real power of the density matrix. Ordinarily, there may be a quantum uncertainty as to the state of the system. Take the example of the spin up or down electron mentioned earlier. We may have the quantum state where the particle has angular momentum in the positive x direction, $|\uparrow_x\rangle = \frac{1}{\sqrt{2}}(|\uparrow\rangle + |\downarrow\rangle)$, so the density matrix is:

$$\rho = \begin{bmatrix} \frac{1}{2} & \frac{1}{2} \\ \frac{1}{2} & \frac{1}{2} \end{bmatrix}. \quad (2.22)$$

We can see that there is 50% chance of measuring either spin up or spin down. We can take the physically different situation where we have a classical mixture of states.

Imagine an electron gun that emits 50% of the electrons *in the spin up state* and 50% *in the spin down state*. Again, if we measure the spin of any electron in our mixture, we will have 50% chance of measuring either way. However, this is a physically different situation. Previously with a quantum superposition we could measure at some axis perpendicular to ‘up’ (namely the x direction) and find all the electrons have the same spin. With the classical mixture, a measurement in *any* direction will give 50% probability results. We can define the density matrix for a mixture of n particles each with well defined density matrix ρ_i to be:

$$\bar{\rho} = \frac{1}{n} \sum_{i=1}^n \rho_i. \quad (2.23)$$

We would therefore get a different density matrix representing the second electron gun system:

$$\bar{\rho} = \begin{bmatrix} \frac{1}{2} & 0 \\ 0 & \frac{1}{2} \end{bmatrix}. \quad (2.24)$$

Notice that since each constituent has trace 1 and is Hermitian, so is this density matrix. Physically, the expectation value for any operator should be the expectation value averaged over each particle (i.e. added and divided by n). The expectation value found by equation 2.14b of this density matrix will give the correct result, because the operators are always linear. Also note that the projection operator will work to give the proportion of particles you would expect to find upon measurement in a particular state. The density operator for an ensemble is defined similarly.

The off-diagonal terms in a density matrix tell you how much the system is mixed. If it is a completely mixed state with no quantum superpositions, then it is guaranteed that the off-diagonal terms are zero. They are maximal in a pure quantum state.

2.1.2 Common Photon Fields

Photons are rarely found to be in a Fock state. The form they take in nature may be rather complicated. Here I will discuss several common states of light.

Chaotic States

Perhaps one of the conceptually simplest states that might be found in nature is the *chaotic* or *thermal* state. This is the state that, for a given mean number of photons \bar{n} , has the highest possible entropy. In this state there is no phase information on the field at all. For instance, interferometry is useless with this state, even if monochromatic. The state can be derived simply by maximising the entropy S

$$S = \sum_{n=0} p_n \ln p_n, \quad (2.25)$$

where p_n is the probability of finding the field in that given Fock state, with the constraint on the mean number of photons. For a thermal field, we also know the mean number [44]:

$$\bar{n} = \frac{1}{e^{\hbar\omega/kT} - 1}. \quad (2.26)$$

We could derive p_n , and it is given by:

$$p_n = \frac{1}{1 + \bar{n}} \left(\frac{\bar{n}}{1 + \bar{n}} \right)^n. \quad (2.27)$$

This is the form of the field in mode of frequency ω that is given off by a black body radiator at temperature T . This would give the diagonal terms of the density matrix, the off-diagonal terms would be zero in this completely mixed state. One should note that the ‘phase’ of electromagnetic field is not defined for chaotic states, and if measured would be completely random.

Coherent States

We would like to know about less chaotic fields for use in the lab. We would search for the *best* field, in the sense that it has the most precisely defined phase and amplitude information (it turns out that they are conjugate-variables and there must be a minimum uncertainty product, given by the uncertainty principle). This field is represented by a pure state called the *coherent* state. It is, in a sense, the closest quantum mechanical field to the classical field. A perfect laser might produce light in this state.

It is not obvious how to define such a state. We can do so, however, with the *displacement* operator. Let α be an arbitrary complex number, and define the displacement operator:

$$\hat{D}(\alpha) = \exp(\alpha \hat{a}^\dagger - \alpha^* \hat{a}). \quad (2.28)$$

The exponential and other such functions are defined on operators by the Taylor expansion. This function has a few interesting properties:

$$\hat{D}^\dagger(\alpha) = \hat{D}^{-1}(\alpha) = \hat{D}(-\alpha), \quad (2.29a)$$

$$\hat{a} \hat{D}(\alpha) = \hat{D}(\alpha) [\hat{a} + \alpha], \quad (2.29b)$$

$$\hat{a}^\dagger \hat{D}(\alpha) = \hat{D}(\alpha) [\hat{a}^\dagger + \alpha^*]. \quad (2.29c)$$

We can denote the *coherent state* $|\alpha\rangle = \hat{D}(\alpha)|0\rangle$. This leads us, after some maths, to find some properties of the coherent state. Firstly it is an eigenstate of the field operators, $\hat{a}|\alpha\rangle = \alpha|\alpha\rangle$. So the mean number of particles in the coherent state is:

$$\bar{n} = \langle \alpha | \hat{a}^\dagger \hat{a} | \alpha \rangle = \alpha^* \alpha = |\alpha|^2. \quad (2.30)$$

We can write down the coherent state in terms of the Fock basis:

$$|\alpha\rangle = e^{-\frac{|\alpha|^2}{2}} \sum_n \frac{\alpha^n}{\sqrt{n!}} |n\rangle. \quad (2.31)$$

So the probability of measuring n particles in the coherent state is:

$$p_n = |\langle n | \alpha \rangle|^2 = \frac{\bar{n}^n e^{-\bar{n}}}{n!}. \quad (2.32)$$

The coherent states are not orthogonal. The inner product and amount of overlap of two coherent states is:

$$\langle \beta | \alpha \rangle = e^{-\frac{1}{2}(|\alpha|^2 + |\beta|^2) + \alpha \beta^*}, \quad (2.33a)$$

$$|\langle\beta|\alpha\rangle|^2 = e^{-|\alpha-\beta|^2}. \quad (2.33b)$$

They do become approximately orthogonal as $\beta - \alpha$ becomes very large. They also form an over-complete basis for the Hilbert space. The identity can be resolved by:

$$\frac{1}{\pi} \int |\alpha\rangle\langle\alpha| d^2\alpha = \hat{1}. \quad (2.34)$$

2.1.3 Operator Ordering

One needs to be careful when dealing with the ordering of the field operators, as they do not commute. A few ‘standard’ orderings are commonly used to describe the order of the particles. *Normally ordered* operators occur with the creation operators preceding the annihilation operators. We denote the normal ordering ‘operators’ as:

$$:\hat{a}^{\dagger n}\hat{a}^m: = :\hat{a}^m\hat{a}^{\dagger n}: = \hat{a}^{\dagger n}\hat{a}^m. \quad (2.35)$$

It is very important to note that the quantities lying between the colons are not equal! In some sense, the ordering colons are not very well defined mathematically, but are simply a useful tool, with which to represent. For instance, one may get confused by:

$$:(\hat{a} + \hat{a}^\dagger)^2: = :\hat{a}^2 + \hat{a}\hat{a}^\dagger + \hat{a}^\dagger\hat{a} + \hat{a}^{\dagger 2}: = \hat{a}^2 + 2\hat{a}\hat{a}^\dagger + \hat{a}^{\dagger 2} \neq (\hat{a} + \hat{a}^\dagger)^2, \quad (2.36)$$

where, although the left-hand-side appears to be already normally ordered, it is not once we expand the brackets! However, one could guess the result simply by imagining the field operators commute and writing it down in normal order.

Sometimes we use the notation $:\hat{O}:_N$ to denote that we are using normal ordering. There are other common orderings, such as *antinormal ordering*, where we rearrange the terms with the annihilation operator preceding the field operators:

$$:\hat{a}^{\dagger n}\hat{a}^m:_A = :\hat{a}^m\hat{a}^{\dagger n}:_A = \hat{a}^m\hat{a}^{\dagger n}. \quad (2.37)$$

Another commonly used ordering is called *symmetric ordering*. It is defined as the equal sum of all the permutations of the field operators. For instance, we can write:

$$:\hat{a}^\dagger\hat{a}:_{\text{sym}} = \frac{\hat{a}^\dagger\hat{a} + \hat{a}\hat{a}^\dagger}{2}. \quad (2.38)$$

We note that symmetric ordering has the following property for bosons:

$$:(\hat{a} + \hat{a}^\dagger)^n:_{\text{sym}} = (\hat{a} + \hat{a}^\dagger)^n. \quad (2.39)$$

One could also define anti-symmetric ordering, where each consecutive permutation is given a negative weighting of the previous permutation. This may be useful for fermionic field operators.

2.2 Phase-Space Diagrams of Quantum States

Often one has trouble imagining complicated quantum states, such as coherent states. Fortunately, wave-functions, state vectors and density operators are not the only ways to describe a quantum system. They can also be described by various phase-space functions.

These are numerical functions that can be used to represent the density matrix of the system. Of particular use are *Quasi-Probability Distributions* or QPDs. These use a particular basis, and the value of the function can relate to the probability of measuring the state to be a particular state of that basis - thus the *quasi*-probability. The basis employed is usually an over-complete basis defined over an uncountable range of parameters (e.g. a real or complex number as a parameter). Because they have a domain larger than the Hilbert space of quantum mechanics, the functions representing complicated states may seem easier to interpret. We shall now look closely at a few more common QPDs.

2.2.1 Q , P and Wigner Functions

The Q Function

We can define several functions based on the coherent state. Perhaps the easiest quasi-probability distribution to define and interpret is the Q function:

$$Q(\alpha) = \frac{1}{\pi} \langle \alpha | \hat{\rho} | \alpha \rangle \quad (2.40)$$

Because of the definition of the density operator, we can see $Q(\alpha)$ is always positive. We can interpret $Q(\alpha)$ to be a measure of the overlap of the quantum state with the coherent state $|\alpha\rangle$. In this way, it measures the probability density of finding it in state $|\alpha\rangle$ upon appropriate measurement, and thus can be called a quasi-probability distribution. The factor of π ensures that the Q function is normalised and is derived from the overcompleteness of the coherent state:

$$\iint_{\alpha \in \mathbb{C}} Q(\alpha) d^2\alpha = 1. \quad (2.41)$$

The fact that the maximum overlap with any state is unity allows us to put a restriction on the size of Q :

$$0 \leq Q(\alpha) \leq \frac{1}{\pi}. \quad (2.42)$$

One can also show that the Q function is smooth (continuous and continuous for every derivative). Given $Q(\alpha)$, the density operator is fully described. It is a complete representation of the system, just as is the density operator. The density operator is related to the Q function via the use of the normally ordered characteristic function (see below), and the Q function exists for all possible density operators.

One very useful fact about the Q function is that it can be used to find expectation values of antinormally ordered quantities:

$$\langle \hat{a}^m \hat{a}^{\dagger n} \rangle = \iint_{\alpha \in \mathbb{C}} \alpha^m \alpha^{*n} Q(\alpha) d^2\alpha. \quad (2.43)$$

The Glauber-Sudarshan P Function

There are other ways to describe the density operator in phase space. For instance, Glauber and Sudarshan suggested the use of the P function:

$$\hat{\rho} = \iint_{\alpha \in \mathbb{C}} P(\alpha) |\alpha\rangle \langle \alpha| d^2\alpha. \quad (2.44)$$

The P function is slightly messier mathematically. We can allow negative and singular valued P functions, such as a coherent state. The P function is not well-defined for all density operators. We can see that a (two-dimensional) delta function will produce a coherent state in equation 2.44. The P function, once known, can also be used to determine the expectation value of any normally ordered operator:

$$\langle \hat{a}^{\dagger n} \hat{a}^m \rangle = \iint_{\alpha \in \mathbb{C}} \alpha^m \alpha^{*n} P(\alpha) d^2\alpha. \quad (2.45)$$

The P function is also a complete description of the state, and is equivalent to the density matrix. The P function can be calculated, in practice, by use of the normally ordered characteristic function.

Characteristic Functions

There are several characteristic functions that can be used to describe a density matrix, and like the above QPDs they are complete representations of the system. The ‘characteristic function’ (sometimes called the ‘symmetrically ordered characteristic function’) is defined as:

$$\chi(\eta) = \text{trace} \left[\hat{\rho} e^{\eta \hat{a}^\dagger - \eta^* \hat{a}} \right]. \quad (2.46)$$

We also define the normally and antinormally ordered characteristic functions similarly:

$$\chi_N(\eta) = \text{trace} \left[\hat{\rho} e^{\eta \hat{a}^\dagger} e^{\eta^* \hat{a}} \right], \quad (2.47)$$

$$\chi_A(\eta) = \text{trace} \left[\hat{\rho} e^{\eta^* \hat{a}} e^{\eta \hat{a}^\dagger} \right]. \quad (2.48)$$

Using a well known operator theorem, we can find a relationship between the different characteristic functions. We know

$$e^{\hat{A} + \hat{B}} = e^{\hat{A}} e^{\hat{B}} e^{[\hat{A}, \hat{B}]}, \quad (2.49)$$

which holds when $[\hat{A}, [\hat{A}, \hat{B}]] = [\hat{B}, [\hat{A}, \hat{B}]] = 0$.

From this we can see they are all related quite simply:

$$\chi(\eta) = \chi_N(\eta) e^{-\frac{1}{2}|\eta|^2}, \quad (2.50a)$$

$$\chi_A(\eta) = \chi(\eta) e^{-\frac{1}{2}|\eta|^2}, \quad (2.50b)$$

$$\therefore \chi_A(\eta) = \chi_N(\eta) e^{-|\eta|^2}. \quad (2.50c)$$

These functions relate to the P and Q functions. If we are able to write the density matrix in P representation using equation 2.44, then we can see:

$$\chi_N(\eta) = \iint_{\alpha \in \mathbb{C}} \langle \alpha | e^{\eta \hat{a}^\dagger} e^{\eta^* \hat{a}} | \alpha \rangle P(\alpha) d^2\alpha = \iint_{\alpha \in \mathbb{C}} e^{\eta \alpha^* - \eta^* \alpha} P(\alpha) d^2\alpha. \quad (2.51)$$

This is a Fourier transform relation as the exponent is purely imaginary. We can use the inverse two dimensional Fourier transform to find $P(\alpha)$:

$$P(\alpha) = \frac{1}{\pi^2} \iint_{\eta \in \mathbb{C}} e^{\alpha \eta^* - \alpha^* \eta} \chi_N(\eta) d^2\eta. \quad (2.52)$$

We can do a similar thing for the Q function. Using the overcompleteness relation of the coherent states (equation 2.34), we can write:

$$\begin{aligned}\chi_A(\eta) &= \text{trace} \left[\hat{\rho} e^{\eta^* \hat{a}} e^{\eta \hat{a}^\dagger} \right] \\ &= \iint_{\alpha \in \mathbb{C}} \frac{\langle \alpha | e^{\eta^* \hat{a}} \hat{\rho} e^{\eta \hat{a}^\dagger} | \alpha \rangle}{\pi} d^2 \alpha \\ &= \iint_{\alpha \in \mathbb{C}} e^{\alpha \eta^* - \alpha^* \eta} Q(\alpha) d^2 \alpha.\end{aligned}\quad (2.53)$$

Again we are left with a Fourier relationship. Thus we can see a second relationship to get the Q function from the density operator:

$$Q(\alpha) = \frac{1}{\pi^2} \iint_{\eta \in \mathbb{C}} e^{\alpha^* \eta - \alpha \eta^*} \chi_A(\eta) d^2 \eta. \quad (2.54)$$

The Q function is the Fourier transform of the antinormally ordered characteristic function. Using equations 2.50 we can see that it must be the Gaussian convolution of the P function:

$$Q(\alpha) = \frac{1}{\pi} \iint_{\beta \in \mathbb{C}} P(\beta) e^{|\alpha - \beta|^2} d^2 \beta. \quad (2.55)$$

This is the origin of the ‘nice’ properties of the Q function. Although the P function can behave strangely, when smoothed out by a Gaussian, it becomes a nice, smooth function.

The Wigner Function

Wigner’s phase space density, or the Wigner function, is arguably the most common and well known QPD. It certainly was the first, developed by Eugene Wigner in 1932 [27]. In analogy to equations 2.52 and 2.54, we write:

$$W(\alpha) = \frac{1}{\pi^2} \iint_{\eta \in \mathbb{C}} e^{\alpha^* \eta - \alpha \eta^*} \chi(\eta) d^2 \eta. \quad (2.56)$$

The Wigner function is also a Gaussian convolution of the P function. We can compare equations 2.50 to the above, and see:

$$W(\alpha) = \frac{2}{\pi} \iint_{\beta \in \mathbb{C}} P(\beta) e^{2|\alpha - \beta|^2} d^2 \beta. \quad (2.57)$$

This is a convolution with a Gaussian of width $1/\sqrt{2}$ of that used to find the P function. We can find the Q function from the Wigner function:

$$Q(\alpha) = \frac{2}{\pi} \iint_{\beta \in \mathbb{C}} W(\beta) e^{2|\alpha - \beta|^2} d^2 \beta. \quad (2.58)$$

The Wigner function has not been smoothed out quite so thoroughly, but still follows some quite nice properties. It exists for all density operators. It is always a smooth function. From the previous equation we can see it is normalised

$$\iint_{\alpha \in \mathbb{C}} W(\alpha) d^2 \alpha = 1, \quad (2.59)$$

and it also turns out to be bounded:

$$-\frac{2}{\pi} \leq W(\alpha) \leq \frac{2}{\pi}. \quad (2.60)$$

But most importantly, we can find the expectation value of any symmetrically ordered operators simply, using the Wigner function:

$$\langle : \hat{a}^{\dagger n} \hat{a}^n :_{\text{sym}} \rangle = \iint_{\alpha \in \mathbb{C}} \alpha^m \alpha^{*n} W(\alpha) d^2\alpha. \quad (2.61)$$

Symmetrically ordered operators turn up surprisingly often, especially when calculating the moments of an observable by raising it to a given power. This turns out to be especially useful when dealing with quadrature.

Quadrature

We define the quadrature observables as the following quantities:

$$\hat{X}_1 = \hat{a} + \hat{a}^\dagger, \quad (2.62a)$$

$$\hat{X}_2 = i(\hat{a}^\dagger - \hat{a}). \quad (2.62b)$$

These observables turn out to be useful quantities. If we take the analogy of \hat{a} and \hat{a}^\dagger to be raising and lowering ladder operators of a single particle harmonic oscillator, then the quadrature observables are comparable to the position and momentum operators for the particle in the quadratic potential.

They are conjugate variables and follow a simple commutation relation:

$$[\hat{X}_1, \hat{X}_2] = 2i. \quad (2.63)$$

This leads to a simple uncertainty relation:

$$\Delta \hat{X}_1 \Delta \hat{X}_2 = 1. \quad (2.64)$$

These two quantities can not be precisely known simultaneously. With the electromagnetic field, these two operators correspond closely to the electric field (see equations 2.2). As a single mode of the electromagnetic field advances in time, the phase factors in equation 2.2c serve to rotate the quadrature. We can write, more generally, the rotated quadrature operator, of angle θ , as:

$$\hat{X}(\theta) = e^{-i\theta} \hat{a} + e^{i\theta} \hat{a}^\dagger. \quad (2.65)$$

This rotated quadrature operator follows similar uncertainty relations as the above special cases of $\theta = 0$ and $\theta = \pi/2$. As time advances, there must be a minimum uncertainty shared between the maximum amplitude and the phase of the electromagnetic wave. We can write a more general commutator:

$$[\hat{X}(\theta), \hat{X}(\theta + \pi/2)] = 2i. \quad (2.66)$$

During an experiment one may be able to measure the electromagnetic field. This is equivalent, in a sense, to measuring one of the quadrature observables. When making

this measurement, the result will be chosen from a probability distribution, as per the measurement postulate of quantum mechanics. We can write the probability for measuring the quadrature to between x and $x + dx$, say, as $w(x)dx$. The probability density $w(x)$ is directly related to the expectation value of the operator:

$$\langle \widehat{X} \rangle = \int_{-\infty}^{+\infty} x w(x) dx, \quad (2.67)$$

and furthermore, the statistics of the measurement are given by the moments of $w(x)$, which are related to the expectation value of the operator \widehat{X} :

$$\langle \widehat{X}^n \rangle = \int_{-\infty}^{+\infty} x^n w(x) dx. \quad (2.68)$$

The Wigner function is closely related to the probability distribution of the quadratures. When a quadrature of any angle is raised to any (integral) power, the result is naturally in symmetric ordering. Take for example:

$$\begin{aligned} \widehat{X}(0)^4 = (\hat{a} + \hat{a}^\dagger)^4 &= \hat{a}^4 + (\hat{a}^3\hat{a}^\dagger + \hat{a}^2\hat{a}^\dagger\hat{a} + \hat{a}\hat{a}^\dagger\hat{a}^2 + \hat{a}^\dagger\hat{a}^3) \\ &+ (\hat{a}^2\hat{a}^\dagger + \hat{a}\hat{a}^\dagger\hat{a}\hat{a}^\dagger + \hat{a}\hat{a}^\dagger^2\hat{a} + \hat{a}^\dagger\hat{a}\hat{a}^\dagger\hat{a} + \hat{a}^\dagger\hat{a}^2\hat{a}^\dagger + \hat{a}^\dagger^2\hat{a}^2) \\ &+ (\hat{a}\hat{a}^\dagger^3 + \hat{a}^\dagger\hat{a}\hat{a}^\dagger^2 + \hat{a}^\dagger^2\hat{a}\hat{a}^\dagger + \hat{a}^\dagger^3\hat{a}) + \hat{a}^\dagger^4. \end{aligned} \quad (2.69)$$

The above operator is clearly symmetrically ordered. That is true for all quadrature angles, and for all powers. The expectation values of any symmetrically ordered operator is given by equation 2.61, and thus we can clearly write the expectation value of each power of any quadrature:

$$\begin{aligned} \langle \widehat{X}(\theta)^n \rangle &= \langle (\hat{a}e^{-i\theta} + \hat{a}^\dagger e^{i\theta})^n \rangle \\ &= \iint_{\alpha \in \mathbb{C}} (\alpha e^{-i\theta} + \alpha^* e^{i\theta})^n W(\alpha) d^2\alpha. \end{aligned} \quad (2.70)$$

We can compare this with equation 2.68, rename one variable, and see that:

$$\int_{-\infty}^{+\infty} x_\theta^n w_\theta(x'_\theta) dx'_\theta = \iint_{\alpha \in \mathbb{C}} (\alpha e^{-i\theta} + \alpha^* e^{i\theta})^n W(\alpha) d^2\alpha. \quad (2.71)$$

Now we wish to split the double integral. We can rewrite α in terms of two real numbers:

$$\alpha = (x_\theta + iy_\theta) e^{i\theta}, \quad (2.72)$$

and then substitute into the previous, and rearrange to get:

$$\int_{-\infty}^{+\infty} x_\theta^n w_\theta(x'_\theta) dx'_\theta = \int_{-\infty}^{+\infty} x_\theta^n \left(\int_{-\infty}^{+\infty} W([x_\theta + iy_\theta] e^{i\theta}) dy_\theta \right) dx_\theta. \quad (2.73)$$

This holds for all n . Given that $w_\theta(x_\theta)$ is a smooth, well behaved function, we can reconstruct it from all of its moments. Thus, we can reconstruct it from the above equation, where we notice we can certainly rewrite our dummy variables $x_\theta = x'_\theta$. Thus we can

equate $w_\theta(x_\theta)$ with the term in parentheses:

$$w_\theta(x_\theta) = \int_{-\infty}^{+\infty} W([x_\theta + iy_\theta] e^{i\theta}) dy_\theta. \quad (2.74)$$

This equation can be interpreted quite naturally. It is the formula for the *marginal* of the Wigner function. A marginal is something like projection. The Wigner function is ‘projected’ onto a quadrature axis by adding (integrating) its values in the perpendicular direction. This is easier to visualise, for instance figure 2.1 demonstrates the point.

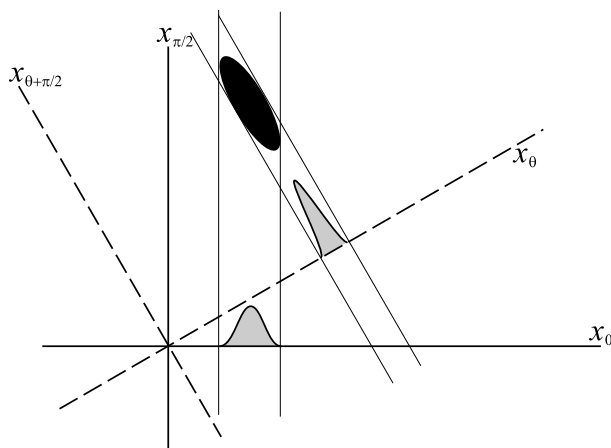


Figure 2.1: This figure demonstrates the idea of marginals. The Wigner function is ‘projected’ onto the quadrature axis by integrating in the perpendicular direction.

This is precisely the reason why the Wigner function is preferred in many areas of physics. The actual values of the Wigner function are extremely closely tied to the probability distributions that are obtainable in reality. In some sense, one might imagine it is plotted on the axes of the quadrature operators themselves.

As time progresses, the Wigner function will change. In the case of the harmonic oscillator potential (as is the case for electromagnetism, see equation 2.4), one can show that the Wigner function simply rotates in time, at the rate of ω (the photon frequency).

Example Wigner Functions

We would like to see the Wigner function for some example state. For instance the coherent state is quite simple to calculate. Obviously, the P function for a coherent state $|\alpha\rangle$ is a delta function centred at α . Using equation 2.57, we quickly arrive at:

$$W_{\alpha_0}(\alpha) = \frac{2}{\pi} \int \delta(\alpha' - \alpha_0) e^{-2|\alpha - \alpha'|^2} d\alpha' = \frac{2}{\pi} e^{-2|\alpha - \alpha_0|^2}. \quad (2.75)$$

Figure 2.2 shows an example of the Wigner function for the vacuum ($\alpha = 0$) and a small coherent state. Note that the vacuum state is radially symmetric - we say it has no *phase information*. As α gets larger, the spread remains constant. Thus, as α gets very large, the Wigner function will become relatively localised to the point α , and the amplitude and phase become extremely well defined (like a classical wave).

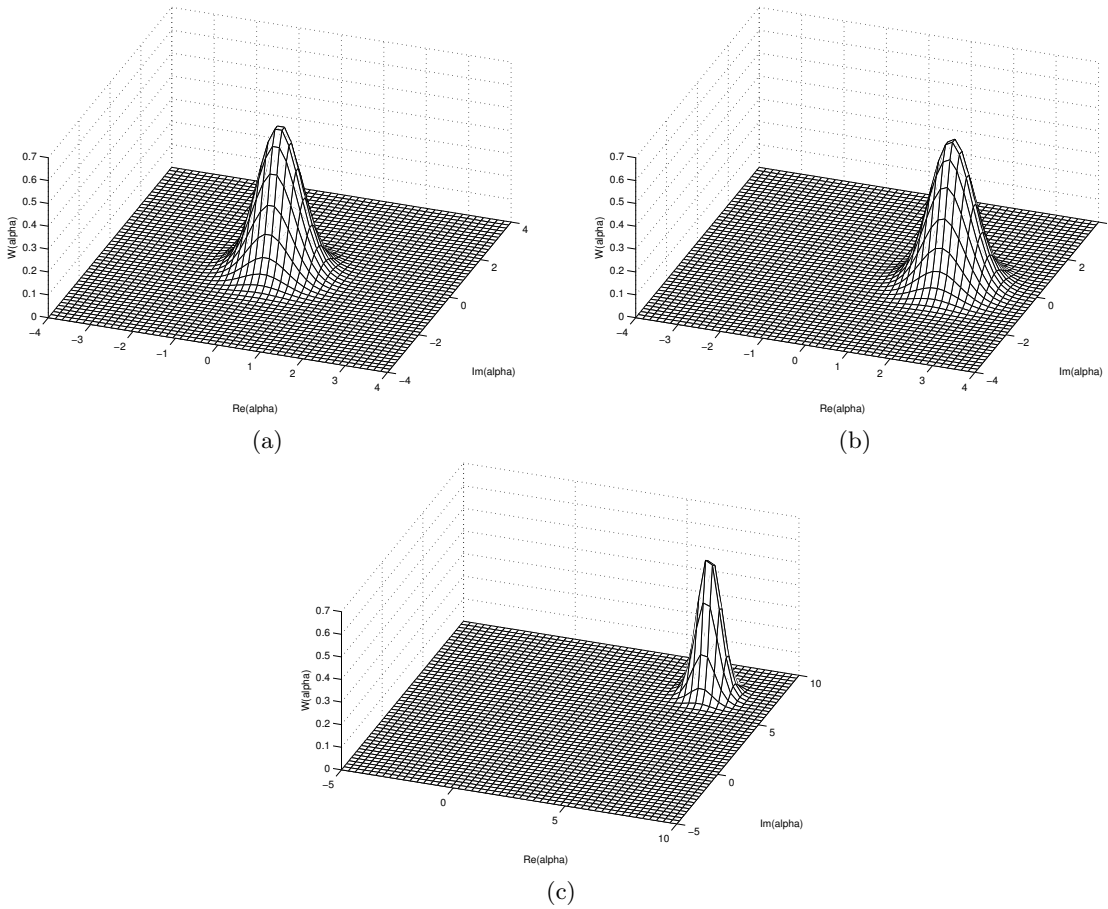


Figure 2.2: The Wigner function plotted for (a) the vacuum, (b) a small coherent state $|2\rangle$, and (c) a large coherent state $|100e^{i\pi/4}\rangle$ (note different scale).

Squeezed and Gaussian States

Now would be a good time to introduce the squeezed state and the generalised Gaussian state. The squeezed state can be defined in terms of the squeezing operator \hat{S} :

$$\hat{S}(\epsilon) = e^{\frac{\epsilon^* \hat{a}^2 - \epsilon \hat{a}^{\dagger 2}}{2}}. \quad (2.76)$$

This is a unitary operator. Essentially this operator will act to decrease the variance in one quadrature, and increase it in another. We write $\epsilon = r e^{2i\phi}$, in which r gives the magnitude of the squeezing, and ϕ gives the quadrature angle which is squeezed (that is, the one where the variance is reduced). The squeezed vacuum states are obtained by applying this operator to the vacuum:

$$|0, \epsilon\rangle = \hat{S}(\epsilon)|0\rangle. \quad (2.77)$$

We can also create displaced squeezed states:

$$|\alpha, \epsilon\rangle = \hat{D}(\alpha)|0, \epsilon\rangle = \hat{D}(\alpha)\hat{S}(\epsilon)|0\rangle. \quad (2.78)$$

These fall into the same family as squeezed displaced states (those with the operators

applied in opposite order) but the value of α used in the displacement operator will be required to change depending on ϵ .

Classical uncertainty in the system may lead to broadening of the Wigner function. The limit of this is the thermal or chaotic state, with the density matrix defined in equation 2.27. This function is radially symmetric and Gaussian in shape:

$$W_{\bar{n}}(\alpha) = \frac{2}{\pi(2\bar{n} + 1)} e^{-\frac{2|\alpha|^2}{2\bar{n}+1}}, \quad (2.79)$$

where \bar{n} is the average number of (chaotic) particles in the system. This state is the most chaotic possible, so it makes sense that the Wigner function contains no phase information. There is no unitary operator to create the chaotic state. Unitary operators can only describe coherent, quantum processes.

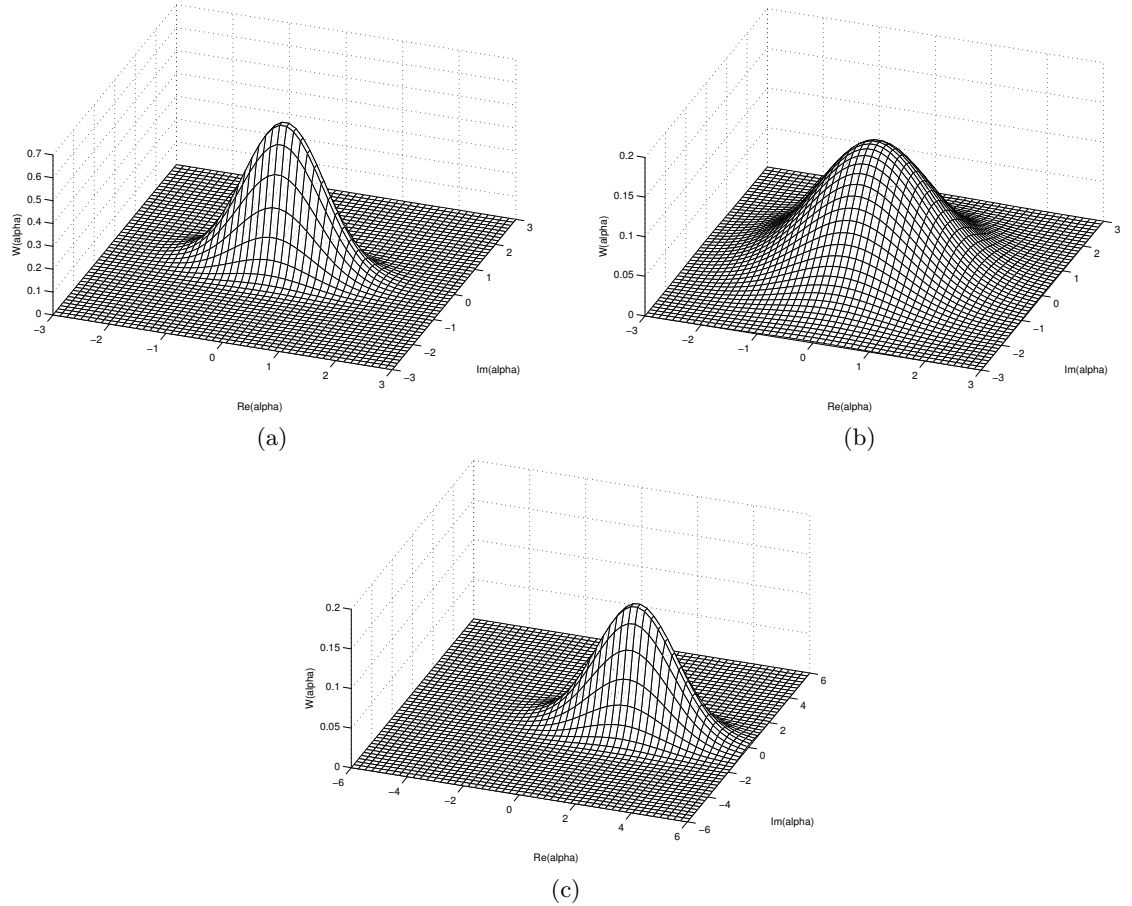


Figure 2.3: The Wigner function plotted for (a) a squeezed state, (b) a chaotic state, and (c) a general displaced, squeezed chaotic state (note different scale).

So far we have seen several different ‘Gaussian’ states (i.e. those with Gaussian shaped Wigner functions). We can create the generalised Gaussian state. These states can either be defined by a normalised Gaussian Wigner function of width obeying the minimum uncertainty relation - the same condition is realised by obeying bounds of the Wigner function in equation 2.60. Alternatively they can be defined as displaced, squeezed chaotic states. That is, we create them by applying the squeezing operator to a chaotic state, and then displace the resulting state. This process will create any physically possible Gaussian

state. Every Gaussian state has non-negative Wigner functions. Conversely, every non-negative Wigner function *representing a pure state* must be a *pure* Gaussian state (i.e. a displaced squeezed state). Sometimes states with non-negative Wigner functions (i.e. Gaussian states) are called classical states - especially in the field of quantum optics.

A few examples of Gaussian states are shown in figure 2.3.

Fock States

The Fock state has a surprisingly complicated Wigner function. It can be shown that it is given by the Laguerre polynomials [44]:

$$W_n(\alpha) = \frac{2}{\pi} (-1)^n L_n(4|\alpha|^2) e^{-2|\alpha|^2}. \quad (2.80)$$

This is a clear example of the Wigner function being negative. Note that these states also have no phase information. Phase is reliant on there being a quantum superposition of number states. In fact, there is an uncertainty relation between the two, however one must be careful to define phase (for a discussion on different phase operators, see [44]).

The Wigner function of several Fock states is illustrated in figure 2.4.

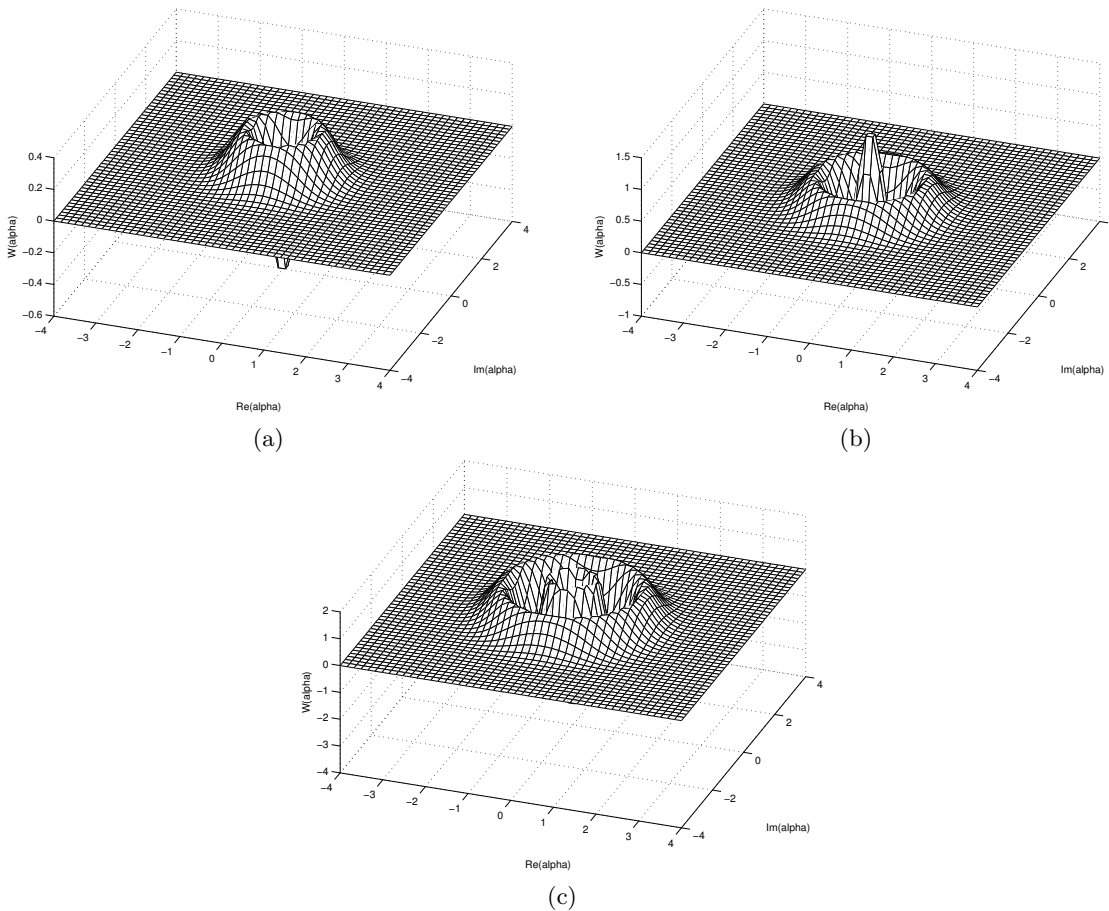


Figure 2.4: The Wigner function of several Fock states: (a) $|1\rangle$, (b) $|2\rangle$, and (c) $|3\rangle$.

Multi-Mode Wigner Functions

We can also write the Wigner function for multi-mode bosonic fields. For a finite number of modes, the Wigner function is expanded in dimensionality. This is needed to compensate for the greatly increased number of states in the product space. For instance, if we have two modes given with field operators \hat{a} and \hat{b} , then we can represent the state as a four-dimensional Wigner function, parameterised by the two ‘complex quadrature variables’ α and β . The Wigner function is written as $W(\alpha, \beta)$. In general, we allow entanglement, so it is not always possible to write:

$$W(\alpha, \beta) = W_{\hat{a}}(\alpha) \times W_{\hat{b}}(\beta) \quad (2.81)$$

The expectation values of symmetrically ordered operators obey obvious relations similar to equation 2.61. All of this extends naturally for any finite number of modes.

2.2.2 The s -parameterised QPD

We have seen that the Q , P and Wigner functions are closely related. In fact, they all fall into the family of the s -parameterised QPD, introduced by Cahill and Glauber in 1968 [28]. We will need to discuss s ordering to explain this function. We begin by writing the s parameterised displacement operator, and expanding:

$$\begin{aligned} \hat{D}(s, \eta) &= \hat{D}(\eta) e^{s|\eta|^2/2} \\ &= e^{\eta \hat{a}^\dagger - \eta^* \hat{a} + \frac{1}{2}s|\eta|^2} \\ &= \sum_{n,m=0}^{\infty} \frac{\alpha^n (-\alpha)^m}{n!m!} \times \{\hat{a}^{\dagger n} \hat{a}^m\}_s. \end{aligned} \quad (2.82)$$

Here we have defined the s -ordered product of $\hat{a}^{\dagger n}$ and \hat{a}^m as the quantity $\{\hat{a}^{\dagger n} \hat{a}^m\}_s$. The exact value of this quantity is defined depending on how the terms of the exponential operator happen to expand. We can compare this equation to the form of the characteristic functions (equations 2.46, 2.47, 2.48) and their relationships (equations 2.50). The case $s = 0$ corresponds to a term in the symmetrically ordered characteristic function, and it can be shown that:

$$\{\hat{a}^{\dagger n} \hat{a}^m\}_{s=0} = : \hat{a}^{\dagger n} \hat{a}^m :_{\text{sym}}. \quad (2.83)$$

We can do the same for the cases $s = \pm 1$, and we find:

$$\{\hat{a}^{\dagger n} \hat{a}^m\}_{s=+1} = : \hat{a}^{\dagger n} \hat{a}^m :_{\text{N}} = \hat{a}^{\dagger n} \hat{a}^m, \quad (2.84)$$

$$\{\hat{a}^{\dagger n} \hat{a}^m\}_{s=-1} = : \hat{a}^{\dagger n} \hat{a}^m :_{\text{A}} = \hat{a}^m \hat{a}^{\dagger n}. \quad (2.85)$$

For the range $0 < |s| < 1$, we can get a feel for how s ordering would work. For positive values, we include all the terms of symmetric ordering in the expansion, but the terms ‘closest’ to normal ordering would be weighted larger than those ‘closer’ to antinormal ordering. The reverse is true for negative quantities.

The s -parameterised characteristic function is given by:

$$\chi_s(\eta) = \text{trace} \left[\hat{\rho} \hat{D}(s, \eta) \right], \quad (2.86)$$

which is compatible with equations 2.46, 2.47 and 2.48.

Then we define the s -parameterised QPD as the Fourier transform of the s -parameterised characteristic function:

$$W(\alpha, s) = \frac{1}{\pi^2} \iint_{\eta \in \mathbb{C}} e^{\alpha \eta^* - \alpha^* \eta} \chi_s(\eta) d^2 \eta. \quad (2.87)$$

Then we can quite clearly see, based on our definitions, that:

$$W(\alpha, 0) = W(\alpha), \quad (2.88a)$$

$$W(\alpha, 1) = P(\alpha), \quad (2.88b)$$

$$W(\alpha, -1) = Q(\alpha). \quad (2.88c)$$

From all of this, we can relate the s -parameterised QPD to expectation values of s -ordered quantities:

$$\langle \{\hat{a}^{\dagger n} \hat{a}^n\}_s \rangle = \iint_{\alpha \in \mathbb{C}} \alpha^m \alpha^{*n} W(\alpha, s) d^2 \alpha. \quad (2.89)$$

The s_1 -parameterised QPD is the Gaussian convolution of the s_2 -parameterised QPD for $s_1 < s_2$. We write:

$$W(\alpha, s_1) = \frac{2}{\pi(s_2 - s_1)} \iint_{\beta \in \mathbb{C}} W(\beta, s_2) e^{\frac{2}{s_2 - s_1} |\alpha - \beta|^2} d^2 \beta. \quad (2.90)$$

The s -parameterised QPDs are well behaved and always exist when s is real and in the range $-1 < s < 1$. The bounds on the functions can be shown to be [28]:

$$|W(\alpha, s)| \leq \frac{2}{\pi(1 - s)}, \quad (2.91)$$

where we note that they may become unbounded in the limit $s = 1$, or the P function. Although the general s -parameterised QPD may not be a good visual tool (with obvious meaning) for non-integral s , it is a useful tool to compute with when performing quantum state tomography.

Literature Review

This chapter constitutes a literature review of the field of quantum state measurement, in particular, applied to BEC. The first section introduces the notion of quantum state tomography, and its application to quantum optics (systems of photons) is reviewed in the second section. A brief review of recent work and understanding of the quantum state of BEC is included in section 3.3. Finally, the last section deals with the concept of the absolute phase reference and the relationship with super-selective Hamiltonians.

3.1 Quantum State Tomography

Ever since the introduction of quantum mechanics, the existence of the quantum wavefunction has been an interesting field of study for physicists. At first glance, one might discard the quantum wavefunction, or state description, as a mathematical tool used to find observable quantities. However, with the use of quantum state tomography, one is able to measure completely the quantum state of a system. Here, we will look at several methods to achieve this.

3.1.1 Single-Particle State Tomography

We can write a Wigner function for a single particle wave function $\psi(x)$. Essentially this consists of converting the complex-valued, real-input wave function into the form of a real-valued, complex input Wigner function. More precisely, we define:

$$W(x, p) = \frac{1}{\pi\hbar} \int_{-\infty}^{+\infty} \langle x + x' | \hat{\rho} | x - x' \rangle e^{2ipx'/\hbar} dx', \quad (3.1)$$

where for a pure state:

$$\hat{\rho} = |\psi\rangle\langle\psi|, \quad (3.2)$$

and a pure state is written in terms of the wavefunction in bra-ket notations:

$$|\psi\rangle = \int_{-\infty}^{+\infty} \psi(x) |x\rangle dx. \quad (3.3)$$

When the Hamiltonian of system is described by the harmonic oscillator, that is:

$$\hat{H} = \frac{\hat{p}^2}{2m} + \frac{1}{2}m\omega^2\hat{x}^2, \quad (3.4)$$

we can solve the system by using the ladder operators [45]:

$$\hat{a}_{\pm} = \frac{1}{\sqrt{2m}} (\hat{p} \pm im\omega\hat{x}), \quad (3.5)$$

where now the Hamiltonian is given by:

$$\hat{H} = \hbar\omega \left(\hat{a}_+ \hat{a}_- + \frac{1}{2} \right) \quad (3.6)$$

A direct analogy can be reached between these ladder operators and the bosonic field operators (equation 2.4). The x - p Wigner function given in equation 3.1 is exactly equivalent to the one given in the previous chapter for the single mode field! We can interpret \hat{x} and \hat{p} as the quadratures of the system, rewriting $W(x, p) = W(x + ip)$. The oscillation in time (of the particle in the harmonic oscillator) is represented by the Wigner function rotating in time at the rate of ω , just as for the electromagnetic case. We can have the equivalent of Fock states (energy eigenstates), vacuum (ground state) and coherent states (minimum-uncertainty wavepackets oscillating in the harmonic potential), and all the other various states that exist.

Although the comparison is strongest with the harmonic oscillator potential, it is not required. Any potential will work and the Wigner function will still have the same meaning with respect to \hat{x} and \hat{p} . However, the evolution of the Wigner function in time will depend on the Hamiltonian.

Experimentally, given an ensemble of particles, one could make measurements of the quadratures \hat{x} and \hat{p} . Given a known symmetry of the system, Kurtsiefer, Pfau and Mlynek [21] were able to reconstruct the Wigner function for an ensemble of helium atoms from a limited number of measurements.

Without any assumed symmetry of the system, a full set (i.e. infinite number) of quadrature angles will need to be measured and processed by the inverse-Radon transformation to obtain the exact Wigner function.

3.1.2 The Inverse-Radon Transformation

Reconstructing quasi-probability distributions by tomographic methods was first proposed by Bertrand and Bertrand [10]. Tomographic methods involve reconstructing a higher dimensional object from lower dimensional marginals, or projections. Following this, Vogel and Risken [11] completed this idea and suggested a method to reconstruct the s -parameterised QPD from the measured quadrature distribution from all angles. If the measurements of the quadrature $\hat{X}(\theta)$ yield the probability distribution $w(x, \theta)$, then we can reconstruct the s -parameterised QPD using the inverse-Radon transformation:

$$W(\alpha, s) = \frac{1}{4\pi^2} \int_{-\infty}^{+\infty} \int_{-\infty}^{+\infty} \int_0^{\pi} w(x, \theta) \exp \left[\frac{s\eta^2}{8} + i\eta \left(x - \frac{\alpha e^{-i\theta} + \alpha^* e^{i\theta}}{2} \right) \right] |\eta| dx d\eta d\theta. \quad (3.7)$$

Although reasonably simple, this equation may be difficult to solve, and may be numerically unstable. Typically, to reconstruct the Wigner function, a very small negative value of s is chosen, in order to make the numerical integration more stable, and the result is assumed to be (very) close to the real Wigner function (for instance, see the method in [26]). Indeed, given equation 2.90, we can see that they will in fact be reasonably close.

3.1.3 Other Reconstruction Methods

There are other methods to reconstruct the quantum state of the system. For example there is the technique of pattern functions [12], and Jaynes' maximum entropy (MAXENT) [13] principle proposed for use in quantum state tomography [14]. When performing quantum state reconstruction, the experimentalist will only be able to measure a finite amount of data. The MAXENT method aims to find the density matrix for the system which matches exactly the experimental data that has been obtained, whilst making as little assumption about the state as possible. This technique has found several applications [15, 16, 17].

3.2 Quantum Optics

Quantum state reconstruction is a technique that has been extensively used in the field of quantum optics. Quantum optics deals with the quantised nature of photons that is inherent in optics. In the quest to learn more about the photon field, many useful experimental and analytic methods have been developed. Quantum state reconstruction is most practical in optical situations as rapidly pulsed or continuous beams allow individual measurements on many 'identically prepared' quantum states to build up the required statistics. Here, we explore some experimental techniques that have been used in order to perform quantum state reconstruction on the photon field.

3.2.1 Direct Detection

We begin with a single spatial mode optical field about which we wish to find information. The simplest optical method of detecting information about the light field is a direct measurement of the intensity of the light beam. This can be achieved by directing the beam onto a photodetector, and we can measure low- and high-frequency fluctuations in the set-up depicted in figure 3.1.

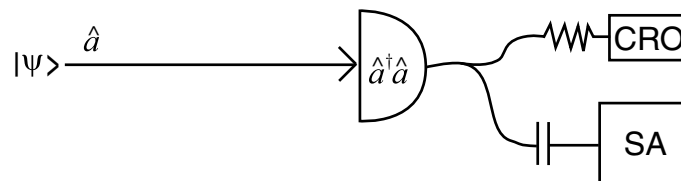


Figure 3.1: Light is incident on a photodetector, which acts as a photon counter. The output is separated into high- and low-frequency components via the use of the capacitor and resistor, and the information is displayed on a spectrum analyser (SA) and cathode ray oscilloscope (CRO), respectively. Light on photodetector connected to resistor-CRO and capacitor-spectrum analyser

The display on the CRO will show the (relatively) long-term averaged intensity of the beam. A real light beam will be made up of a range of frequencies, and interference will cause higher frequency fluctuations that can be viewed by the spectrum analyser.

For a perfectly single mode input field, we can easily find the possible information that can be obtained from this system. The photocurrent detected on the CRO will be proportional to the number of photons incident on the photodiode, and for a perfect

detector we can write the second-quantised equation,

$$\hat{i} = e\hat{a}^\dagger\hat{a}, \quad (3.8)$$

where \hat{a} is the annihilation operator of the given photon field. With a perfect detection system, we could in this way determine the precise number distribution of the field.

A photodetector with quantum efficiency η will produce an average current proportional to the average number of photons. We would partially add vacuum to the field to obtain the operator result, using \hat{u} as a field operator for the vacuum:

$$\hat{a}_{\text{measured}} = \eta\hat{a} + (1 - \eta)\hat{u}. \quad (3.9)$$

We could then obtain the result:

$$\langle \hat{i} \rangle = \eta e \langle \hat{a}^\dagger \hat{a} \rangle. \quad (3.10)$$

At least some information on the detail of the number statistics will survive an imperfect detector. However, with this scheme no ‘phase information’ can be found. That is, from the density matrix of the photon field

$$\hat{\rho} = \sum_{i,j} c_{ij} |i\rangle\langle j|, \quad (3.11)$$

we can find the diagonal terms c_{ii} , but *no* information on the off-diagonal terms.

3.2.2 Standard Homodyne Detection

To find more information about the light field, the field of quantum optics developed the technique of homodyne detection. The quantum theory of photons replaces classical travelling electromagnetic waves, and there must be an analogy which allows us to measure the amplitude of the electric field, not just the intensity of the wave. We are able to achieve this through a homodyne measurement, which is essentially an interference experiment between the field we are interested in and another field that acts as a fixed phase reference (called a ‘local oscillator’). Through this we are able to measure a *quadrature* of the field (see section 2.2). The schematic for standard homodyne detection is depicted in figure 3.2.

We begin with an input field with annihilation operator \hat{a} , and mix it on a beam splitter with a *phase locked* reference field with field operator \hat{b} . Assuming we are performing balanced homodyning (i.e. using a 50-50 beam splitter), in the Heisenberg picture we can find the resulting field operators.

$$\hat{c} = \frac{\hat{b} + i\hat{a}}{\sqrt{2}} \quad \hat{d} = \frac{\hat{a} + i\hat{b}}{\sqrt{2}} \quad (3.12)$$

The current that is measured is the subtracted current between the photodetectors. Under a perfect measurement scheme we can find this difference:

$$\hat{i}_- = e \left(\hat{c}^\dagger \hat{c} - \hat{d}^\dagger \hat{d} \right) = e i \left(\hat{b}^\dagger \hat{a} - \hat{a}^\dagger \hat{b} \right). \quad (3.13)$$

Now we must use the fact that \hat{b} is being used as a phase reference. Some states have quasi-probability distributions found a long way from the origin, localised around a certain

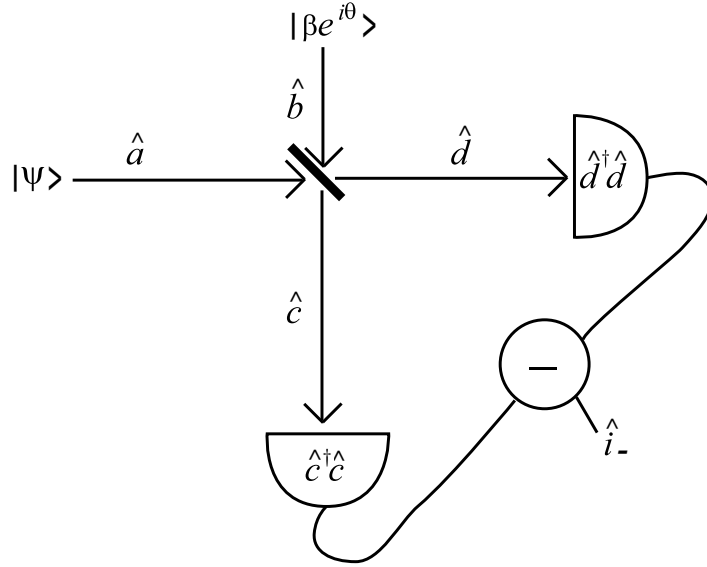


Figure 3.2: A standard balanced homodyne scheme consists of a 50-50 beam splitter combining two optical fields, which are then detected by two photo detectors. The subtracted current is used to find quadrature information.

point. An example of this is a large coherent state, $|\beta e^{i\theta}\rangle$, say. In this case we can linearise the operator:

$$\hat{b} = \beta e^{i\theta} + \hat{d}b. \quad (3.14)$$

The second term is much smaller than first. Upon measurement, this will fluctuate about a size of $\sqrt{\beta}$ for a coherent state. Given the typical size of photonic fields, this will be several orders of magnitude smaller.

Given a largely displaced field, then we are measuring:

$$\hat{i}_- = e\beta i \left(\hat{a}e^{-i\theta} - \hat{a}^\dagger e^{i\theta} \right) + \text{order} \left[e \hat{d}b \right] \approx 2e\beta \hat{X}(\pi/2 - \theta). \quad (3.15)$$

where $\hat{X}(\phi)$ is the rotated quadrature operator as discussed in section 2.2, and defined in equation 2.65.

Before we continue, we must first note two things. Firstly, and most importantly for this thesis, is the fact that we required the local oscillator to be phase-locked with the source. That is, the local oscillator field must be ‘local’ in the sense that it is already entangled in some way with the field we are going to measure. Experimentally, this requirement could be achieved by beginning with a single laser beam, splitting a piece off and manipulating it to form our input field. The remainder of the laser beam is used as the local oscillator. This ensures that the phase of the local oscillator is fixed with regards to the input beam as time goes on. If this were not the case, and the phase was randomly changing between measurements, the quadrature measurement would be ‘washed-out’ over all angles and again we would be left with no phase information.

The second thing to note is a technical problem for optical fields. Typically, in these experiments, one measures the side-bands of the laser (slightly different frequencies from the average frequency of the beam). If this scheme were used with a spectrum analyser, as indicated, we could not get all the statistical information of the field [26]. We would find

the average and variance, however, and this would be enough to reconstruct Gaussian fields (i.e. those fields with Gaussian shaped Wigner functions). Full reconstruction experiments in quantum optics are done using a slightly more sophisticated method.

3.2.3 Optical Homodyne Tomography

To measure side-band correlations on a laser beam, one would have to use a slightly more complicated method to those mentioned so far. One solution is to use the technique of optical homodyne tomography (OHT), which has been used extensively in quantum-optics experiments [18, 19, 20, 26]. In OHT experiments, not only is the relative phase of the central frequency to the local oscillator known, but also the phase of the modulated side-bands is taken account of after detection. In this way, one is able to separate the quadrature observable that one is interested in. A typical OHT set-up is shown in figure 3.3.

The local oscillator is first split off and the phase (θ) is controlled by the piezo-electric device on the back of the mirror. The other beam will be modified by the experimentalist, for instance this set-up includes amplitude- and frequency-modulation. The phase of this modulation is delayed by ϕ . Modifying θ or ϕ will change the quadrature angle measured. However, the amplitude of the measured quadrature depends on values of θ and ϕ . By controlling these two values, the experimentalist is able to maintain constant amplitude whilst still changing the quadrature angle. For a partially semi-classical derivation of this system, see [26].

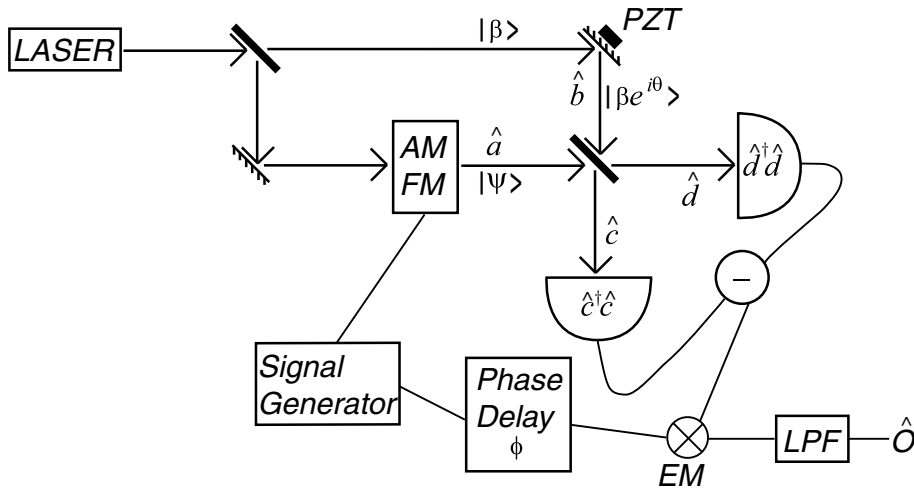


Figure 3.3: The experimental set-up used in OHT experiments. The phase of the modulation is delayed by ϕ before mixing occurs in order to control quadrature angle. AM/FM: amplitude- and frequency-modulator, PZT: piezo-electric transducer, EM: electronic mixer, LPF: low-pass filter.

Using this method, the experimenter is measuring precisely the effects on the field that was put on by the modulators. It is hard to consider that it is measuring much information about the field that was there before the initial beam splitter, except that we make the assumption that it is ‘close’ to a large coherent state in order to linearise the field.

Once this is complete for all quadrature angles, the experimenter would then have to perform reconstruction of a quasi-probability distribution. The inverse-Radon transformation would then be applied to the data to create the Wigner function. Surprisingly,

the inverse-Radon transformation is not necessarily an easy step. Often, one will notice ‘ripple’-like artefacts on the resulting Wigner function due to imperfect measurement and reconstruction.

3.2.4 Self-Homodyne Tomography

So far, we have required the use of a second ‘phase-reference’ beam to reconstruct the quasi-probability distributions. We shall now discuss a technique, useful in quantum optics experiments, titled self-homodyne tomography. Using this scheme, experimentalists have been able to remove the requirement of a second, phase-locked reference beam [24].

This technique is strictly for use with multi-mode fields. The term *self*-homodyne is slightly misleading - a strongly coherent frequency is still required. It is, however, already included in the spatial mode of the beam. It can be applied, for example, to measure side-band squeezing around a strong coherent central frequency. In essence, the different frequencies are phase shifted relative to one another, creating a method to measure each different quadrature.

We shall look at a self-homodyne tomography method employed by several groups [22, 23, 24] involving the use of a single-ended Fabry-Pérot resonator. A simplified version of the experimental set-up is depicted in figure 3.4.

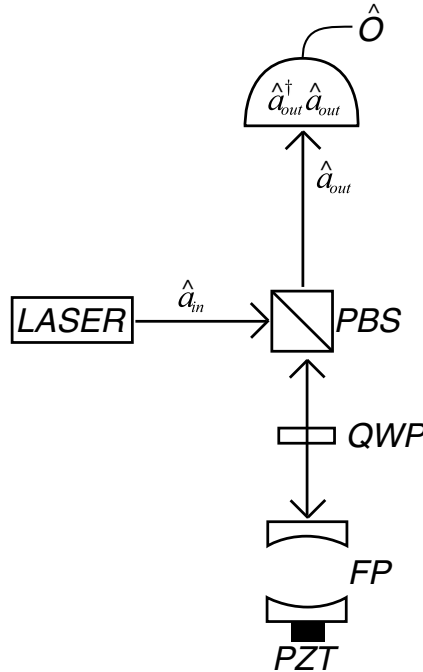


Figure 3.4: A simplified experimental set-up used for self-homodyne tomography. The length of the cavity is changed in order to modify the quadrature angle measured at \hat{O} . PBS: polarising beam splitter, QWP: quarter-wave plate, FP: Fabry-Pérot resonator cavity, PZT: piezo-electric transducer.

The polarising beam splitter and quarter wave plate act as an optic circulator. The light going into the Fabry-Pérot comes entirely from the laser, and the light leaving the Fabry-Pérot is entirely diverted to the detector.

The Fabry-Pérot has a classical effect on the electric field. Classically, we write:

$$E_{\text{out}}^+(\omega) = F(\omega)E_{\text{in}}^+(\omega). \quad (3.16)$$

Quantising the electric field, using \hat{a} as the photon annihilation operator, we have [47]:

$$E_{\text{in}}^+(\omega) \equiv \sqrt{\frac{\hbar}{2\epsilon_0}} \hat{a}_{\text{in}}(\omega). \quad (3.17)$$

In general we would need to use a unitary operator to investigate the effect of the resonator, but luckily a simple resonator is quite simple. Under the assumption that $|F(\omega)| = 1$ (i.e. no photons in any mode are created or destroyed, such as a lossless resonator - see [24] for an analysis of loss), we can apply equation 3.16 to get

$$\hat{a}_{\text{out}}(\omega) = F(\omega)\hat{a}_{\text{in}}(\omega), \quad (3.18)$$

where

$$F(\omega) = \frac{1 - i\theta(\omega)}{1 + i\theta(\omega)}, \quad (3.19)$$

and $\theta(\omega) = (\omega_c - \omega)/k$ is the detuning of ω from the nearest cavity resonance ω_c , normalised to the half line-width of the cavity k [24]. Next we shall analyse the output of a detector with multi-mode input.

Multi-mode Detection

We begin with a particle detector measuring a multimode field. It takes a measurement as a function of time, thus the output is:

$$\hat{O}(t) = \hat{a}^\dagger(t)\hat{a}(t). \quad (3.20)$$

We should be careful to define the relationship between the operators in time and frequency domains:

$$\hat{a}(t) = \frac{1}{\sqrt{2\pi}} \int_{-\infty}^{+\infty} \hat{a}(\omega)e^{-i\omega t}d\omega, \quad (3.21a)$$

$$\hat{a}(\omega) = \frac{1}{\sqrt{2\pi}} \int_{-\infty}^{+\infty} \hat{a}(t)e^{i\omega t}dt, \quad (3.21b)$$

$$[\hat{a}(\omega)]^\dagger = \hat{a}^\dagger(-\omega). \quad (3.21c)$$

We wish to look at the frequency information of the output, so we take the Fourier transform and apply the convolution theorem:

$$\begin{aligned} \hat{O}(\omega) &= \frac{1}{\sqrt{2\pi}} \int_{-\infty}^{+\infty} \hat{a}^\dagger(t)\hat{a}(t)e^{i\omega t}dt \\ &= \frac{1}{\sqrt{2\pi}} \int_{-\infty}^{+\infty} \hat{a}^\dagger(\omega')\hat{a}(\omega - \omega')d\omega'. \end{aligned} \quad (3.22)$$

Next we assume that we are working with a very large central frequency ω_0 . We

separate out the large component at that frequency by writing:

$$\hat{a}(\omega) = \alpha\delta(\omega_0) + \hat{d}a(\omega). \quad (3.23)$$

Rewriting the output with this substitution yields:

$$\begin{aligned} \hat{O}(\omega) = & \frac{1}{\sqrt{2\pi}} \left[|\alpha|^2\delta(\omega) + \alpha\hat{d}a^\dagger(\omega - \omega_0) + \alpha^*\hat{d}a(\omega + \omega_0) \right. \\ & \left. + \int_{-\infty}^{+\infty} \hat{d}a^\dagger(\omega')\hat{d}a(\omega - \omega')d\omega' \right]. \end{aligned} \quad (3.24)$$

If we assume that, in some sense, $\alpha \ll \hat{d}a(\omega)$, then we can see that the last term is negligible. For frequencies other than zero, the first term is zero. If we measure a frequency $\Omega \neq 0$ and ignore the other frequencies, and write $\alpha = |\alpha|e^{i\theta}$, we therefore have

$$\begin{aligned} \hat{O}(\Omega) & \approx \frac{|\alpha|}{\sqrt{2\pi}} \left(e^{-i\theta}\hat{d}a(\omega_0 + \Omega) + e^{i\theta}\hat{d}a^\dagger(\Omega - \omega_0) \right) \\ & \equiv \frac{|\alpha|}{\sqrt{2\pi}} \hat{X}_\Omega(\theta), \end{aligned} \quad (3.25)$$

which is proportional to the sideband quadrature, defined similarly to the single mode quadrature in section 2.2. This observable measures correlations between different modes (frequencies) of the photon field. The quadrature angle is defined by the central frequency's phase θ . In quantum optics experiments, the sidebands are often created from the central frequency, and so α can not be changed without changing how the sidebands are created.

In reality we can not measure this non-Hermitian operator, $\hat{O}(\Omega)$, exactly, only some phase component of it. We would achieve this experimentally by electronically mixing the output signal with an electronic local oscillator of frequency Ω . The phase of the local oscillator will determine the complex phase of the above frequency that is measured. For zero phase, say, we measure the real part $\hat{O}(\Omega) + \hat{O}(-\Omega)$. Note that this is an Hermitian observable, as $\hat{O}(t)$ is Hermitian.

Using the Fabry-Pérot

We now wish to see the effect of the Fabry-Pérot resonator on the output given by equation 3.25. By substituting equation 3.18 into equation 3.23, we arrive at the following transformation.

$$\hat{d}a_{\text{out}}(\omega) = F(\omega)\hat{d}a_{\text{in}}, \quad (3.26a)$$

$$\alpha_{\text{out}} = F(\omega_0)\alpha_{\text{in}}. \quad (3.26b)$$

Substituting these values back into equation 3.25, we see that:

$$\hat{O}(\Omega) \approx \frac{|\alpha|}{\sqrt{2\pi}} \left(e^{-i\theta}F^*(\omega_0)F(\omega_0 + \Omega)\hat{d}a(\omega_0 + \Omega) + e^{i\theta}F(\omega_0)F^*(\omega_0 - \Omega)\hat{d}a^\dagger(\Omega - \omega_0) \right). \quad (3.27)$$

Depending on the behaviour of $F(\omega)$, we can see that the phase difference between the two terms can be controlled. In experiments such as [24], one controls the behaviour of $F(\omega)$ by means of a piezoelectric transducer on one mirror of the cavity. By changing the location of the nearby resonating frequency, we can see that F can change rapidly. Thus,

with careful analysis of the results, one can conclude which quadrature is being measured, change quadrature angle, and ultimately reconstruct the quantum state.

3.3 The State of BEC

Previously, physicists have attempted to study the state of dilute-gas BECs. There has been much debate as to what sort of state it might start in. It may in fact be in a fixed number state (with some classical uncertainty due to the experimental apparatus), or a coherent state where it is in a superposition of number states, or some other state altogether. The idea of there being a quantum uncertainty in the number of atoms in the BEC is not as absurd as it might seem. Each individual atom could be in a superposition of being in the trap and outside the trap. Thus, if we are looking at just the atoms inside the trap, we find that there is strictly quantum uncertainty in the number. In this system, measuring the number of atoms outside the trap will collapse the number inside (to within whatever classical uncertainty the system might possess).

This section outlines some of the theoretical and experimental work in this area. It is a summary of Tom Hanna's literature review and report [46], and of an interesting paper by Mourtizen and Mølmer [17].

3.3.1 Theoretical Progress

Theorists have attempted to find experimental methods in order to prove what type of state a BEC might start in. We must, however, be extremely careful how we define our system. The definition of phase in the system is also another important point.

Single BECs

The first result applies to single BECs. We do not have an *absolute phase reference* (see section 3.4) for atoms. The 'phase' of a single set of atoms is not well defined. We can, of course, *write down* a state with defined phase - but relative to what?

Let us begin with a state of well defined phase, for instance a coherent state $|\alpha\rangle$. However, we are unsure of the absolute phase for this state. We can say that there is a classical uncertainty in the absolute phase. We can write the density matrix for the system:

$$\hat{\rho} = \int_0^{2\pi} |\alpha e^{i\phi}\rangle \langle \alpha e^{i\phi}| \frac{d\phi}{2\pi}. \quad (3.28)$$

In the Fock basis it can be shown that the off-diagonal terms of the density matrix are zero. The diagonal terms give the number statistics, which are independent of phase. Thus the number statistics are the same as for a coherent state, that is, a Poissonian distribution (a result derived in [29]).

Therefore, we can see that the density matrix is the same as a classical mixture of Fock states:

$$\hat{\rho} = \sum_{n=0}^{\infty} \frac{|\alpha|^{2n} e^{-|\alpha|^2}}{n!} |n\rangle \langle n|. \quad (3.29)$$

The Fock states have no defined phase what-so-ever. The density matrix fully describes the system, and we have seen that uncertain absolute phase is exactly equivalent to Fock states of uncertain number. The system described above can have no detectable phase information.

The problem at hand is that we can only measure relative phase. In section 4.1 this is dealt with more thoroughly.

Multiple BECs

With the single-BEC problem resolved, theorists next moved on to looking at multiple BECs, and what can be achieved by interfering two or more BECs. First, we shall look at what occurs when two BECs interfere. In a typical experiment, we would begin with two BECs with zero overlap. Ideally, the experimentalist would then expand the two BECs into two plane waves, which would then be detected on a screen (figure 3.5). Detections occur as each atom leaves a ‘click’ on the screen. Eventually, when the relative phase is well defined, interference fringes will appear.

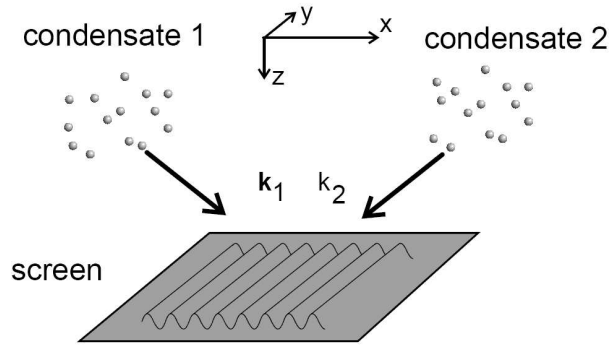


Figure 3.5: Two spatially separated BECs are expanded into plane waves, and interfere on the detection screen. Picture from [30].

The measurements in this experiment are clearly quantum measurements. As such, they are able to change the state that is being measured. For instance, we already know that two Fock state BECs have no pre-defined relative phase as neither has any phase information (because they have certain number). As particles are detected, we are unsure of which BEC the particle originated from. Thus, the particle number of each BEC becomes uncertain. Each BEC may begin to build up phase information, and an interference pattern emerges (with a randomly selected phase). Note that the total particle number of the two BECs *is* certain throughout the experiment.

We may also begin the experiment with two coherent states. These coherent states may each have unknown absolute phase, and unknown relative phase. We could write this state down as:

$$\hat{\rho} = \int_0^{2\pi} \int_0^{2\pi} |\alpha e^{i\phi}\rangle \langle \alpha e^{i\phi}| \otimes |\beta e^{i\psi}\rangle \langle \beta e^{i\psi}| \frac{d\psi}{2\pi} \frac{d\phi}{2\pi}, \quad (3.30)$$

where both phases are unknown. Similarly to the single-BEC result, this has the same density matrix of a classical mixture of Fock states in each BEC. Interference is established by exactly the same mechanism as in the previous paragraph, and the relative phase measured will have a completely random result.

However, we can have a *relative phase coherent state*, as defined in [31], where we write the density matrix as:

$$\hat{R}_{\alpha\beta}(\phi) = \int_0^{2\pi} |\alpha e^{i\phi'}\rangle \langle \alpha e^{i\phi'}| \otimes |\beta e^{i(\phi'-\phi)}\rangle \langle \beta e^{i(\phi'-\phi)}| \frac{d\phi'}{2\pi}. \quad (3.31)$$

With this state the relative phase is well defined. Integrating this over all ϕ will

yield the density matrix in equation 3.30. The interference measurement constitutes a measurement of the relative phase. After measurement of some atoms the unknown relative phases state will begin to approach the relative phase state above. Although the phase may be known after only a few detections, a ‘significant fraction’ [32] of the atoms will be required to be measured before the state has a large overlap with the state in equation 3.31.

Some researchers have looked at the development of the visibility of the fringes [33]. The visibility is the same for Fock states and Poissonian mixtures of Fock states (i.e. unknown phase coherent states), and so we can not tell the difference between the two. However, states with broader number distribution, such as chaotic states, have less visibility. The chaotic state has visibility $\pi/4$, for instance.

Work has been done on many BECs in an optical lattice, and phase relationships between lattice sites [34, 35].

Collisions

The effect of collisions in the BEC on phase and relative phase has been studied. Elastic collisions in BEC essentially change the energy of the system, and thus the rate with which the phase rotates in time. Inelastic collisions can have a more complicated result, often adding classical uncertainty to the system and removing phase information. Either way, the relative phase between two systems is expected to become less well-defined due to collisions as time goes on [36, 37, 38]. Many groups have predicted ‘phase revivals’, where the mechanism that causes the phase to diffuse goes full circle, and the phase becomes well-defined again. Inelastic collisions will dampen the strength of the revival [38].

3.3.2 Experimental Results

Many groups around the world are now able to produce BECs, and many of them are able to create multiple BECs. This is usually done either in a double well trap (such as those possible with time-orbiting potentials), or in optical lattices.

The coherent evolution of relative phase between BECs was first demonstrated in 1997 [39], and more accurate results were obtained in 2003 [40]. In these experiments, the experimentalist was able to control the relative phase between the BECs, for instance by using the Stark shift. This was seen to be the first evidence of phase existing and being well-defined for a BEC.

A lot of recent work has focused on optical lattices. Several groups have observed phase collapse and revival in their experiments [41]. There is still debate on the meaning of results of some experiments. For a more comprehensive review of recent experimental results I recommend [46].

3.3.3 Perturbed BEC

An interesting paper was written recently by Mouritzen and Mølmer [17]. They have attempted to analyse (computationally) the effect of different types of perturbations to an untrapped BEC. Assuming the experimenter could make certain measurements, they employed the MAXENT principle (see section 3.1.3) to reconstruct the quantum state of the system. They used the Gröss-Pitaevskii approach to model the dynamics of the BEC, and used a Bogoliubov approximation with the MAXENT principle to find their results.

They found that the reconstructed density operator gave excellent predictions on some quantities - such as the second moments of the annihilation and creation operators. By including further measurements (of the momentum), they could correctly differentiate between coherent and thermal states. Note that these are states of perturbations in the Bogoliubov transformation. Finally, by assuming a measurement on the zero-wave-number (unperturbed part) of the ‘anomalous second moment’, $\langle \hat{a}_0^2 + \hat{a}_0^{\dagger 2} \rangle$, they were able to make reliable predictions on the anomalous second moment in the position basis - and thus they claim they could measure amplitude squeezing in the position basis of the BEC.

3.4 Absolute and Relative Phase References

We, as humans, have the technology to create and destroy photons at will. For instance, we are able to create lasers that create a source of photons in a state close to a coherent state. However, we can not do the same for matter. Although we have caused creation in the form of pair production in particle physics experiments, this is certainly not a coherent and deterministic process. I could not imagine being able to cause the creation of a coherent set of electrons and positrons - let alone the coherent creation of a bound atom such as ^4He (and its anti-particle).

At the energy scale used in atom optics, there is a negligible chance that the nucleus of an atom will become unbound. Without any approximation, a term in the system’s Hamiltonian will exist that allows this possibility. However, we would chose to ignore this term because its effect would be almost infinitesimal. However, photons could be absorbed and emitted by the atoms, and thus we can not ignore the possibility of creation or annihilation of photons.

This idea is described in terms of super-selection rules. Super-selection rules limit the possible terms that can appear in the Hamiltonian. For instance, if we know the number of atoms in the system is conserved, then the Hamiltonian must respect that. Terms like the number operator, $\hat{a}^\dagger \hat{a}$, will never change the number of particles in a state. That operator has the effect of annihilating then creating a particle. On the other hand, the Hermitian operator $\hat{a} + \hat{a}^\dagger$ does not conserve number. This operator represents the possibility of annihilating a particle *or* creating a particle.

For multi-mode fields, we may allow the particle to be annihilated in one mode, and created in another - thus conserving total particle number. If \hat{a} and \hat{b} are the annihilation field operators of two modes of atoms, say, then the Hermitian operator $\hat{a}^\dagger \hat{b} + \hat{a} \hat{b}^\dagger$ represents this possibility.

We say an operator is *quadratic* if each term has the same number of creation and annihilation operators. In atom optics, we would therefore expect a Hamiltonian to be quadratic in the atomic field operators, but not necessarily in the photon operators.

The conclusion reached is that we are able to create an ‘absolute phase reference’ with the photons (actually, by absolute I mean as absolute as physically possible, i.e. ‘an agreed time standard’, as discussed in [42]). In theory, with the allowed Hamiltonian we are able to create a photonic source (like a coherent laser) that we are able to directly use as a ‘clock’. With this ‘clock’, we have accurate time resolution to the frequency of the photons. We could, theoretically, *directly* observe the oscillating electric field at optical frequencies! However, due to limited technology, we are only able to do this for lower frequency photons (radio frequencies).

However, we can *not* do the same with the atoms. In quantum mechanics, the phase rotates at rate $\omega = E/\hbar$, where E is the total energy of the particle - including mass energy.

For slow-moving ^4He , this equates to a frequency of $f \approx 9 \times 10^{23}$ Hz. Given super-selection on the atomic field (and indeed all fields of this energy scale), we are completely unable to directly measure the phase of the atoms. However, we can measure *relative phase* between two atomic sources because we can interfere them and measure the beating which occurs at much lower frequencies.

For a more comprehensive discussion on this topic, see Wiseman's paper [42] and its dependencies.

Detection of BEC

The results found during the course of this thesis are outlined in this chapter and the following two. This chapter looks primarily at the measurement of quantum statistics relevant to BECs. The first half of this chapter finds limitations on what information about a single-mode field can be measured. The second half (section 4.2) deals with the implications of those limitations on BEC, and outlines some other results pertinent to the detection of quantum statistics in a BEC.

4.1 Single-Mode Detection

In this section we deal with the detection of single-mode bosonic fields. Because in atom-optics experiments the atom number is conserved, we find we are lacking an absolute phase reference (section 3.4). It is shown that this severely limits what is measurable in an atom-optics experiment. Measurement of the quadrature operator of a single mode of the field may be impossible under these conditions.

4.1.1 Single-Mode Closed Systems

First we begin by analysing the simplest imaginable system, to see what we are able to detect. Imagine a perfectly single mode collection of bosons (such as a zero temperature BEC) in state $|\psi\rangle$ with field annihilation operator \hat{a} , and that this is the only field that we have access to.

We know that experimentally we can only detect the statistics of the operator $\hat{a}^\dagger\hat{a}$. This is the number operator, which is obvious that we can measure. However we can not *directly* measure things of the form $\hat{a}e^{i\theta} + \hat{a}^\dagger e^{-i\theta}$ with any detection method that we are aware of. This is not to say that it is not measurable at all, but in order to do so we need to interact the system with another field. However, we have assumed the system is closed and does not interact with any fields (except those in the simple particle counter).

Thus we must come to the conclusion that in this restricted system it is impossible to ever measure the exact quadrature components and thus reconstruct the quantum state. However we do get half of the quantum information - the number statistics - but not the phase information. If we write

$$|\psi\rangle = \sum_{n=0}^{\infty} c_n |n\rangle, \quad (4.1)$$

then we can measure the modulus of each c_n but not the argument. The best we could do is assume the system is in a mixed state where the argument of each c_n is completely unknown. In the quasi-probability distribution picture, this is equivalent to detecting

‘radial’ information, but no ‘angular’ (or phase) information.

4.1.2 Measuring with Vacuum?

In reality, a single mode of the field will be able to interact with surrounding modes. A number of modes in various states may surround the one in question. We now consider a slightly more realistic system than the previous, and find that the quadrature observable may still not be available to measure. Many modes and more complex states will be dealt with later in the chapter.

We begin with the same single mode system and allow it to couple to a single mode vacuum state. The quantum state thus begins as $|\psi\rangle \otimes |0\rangle$ and we have the first mode’s annihilation operator \hat{a} and the annihilation operator of the vacuum \hat{b} .

We now also impose the ‘super-selection’ condition on our closed system where the boson number is conserved. This is a very accurate description when dealing with atoms as they can not be created and destroyed at the relevant energy scales (this may not be true for *metastable* helium, this will be discussed in section 4.2.1). This super-selection rule will ultimately limit the form that the Hamiltonian can take. The Hamiltonian can entangle the two modes together and will be of the general form:

$$\hat{H}(t) = \sum_{m+n=p+q} c_{mnpq}(t) \hat{a}^{\dagger m} \hat{b}^{\dagger n} \hat{a}^p \hat{b}^q, \quad (4.2)$$

where $c_{pqmn}(t) = c_{mnpq}^*(t)$ as the Hamiltonian is Hermitian.

Notice that the total number of annihilation operators in each term equals the number of creation operators (sometimes referred to as *quadratic* terms). Thus the Hamiltonian always acts to conserve the total number of particles in the system. After a time t_0 of evolution under the Hamiltonian, we can find the unitary operator which describes the evolution of the system with the well known equation:

$$\hat{U}(t_0) = \exp\left(-\frac{i}{\hbar} \int_0^{t_0} \hat{H}(t) dt\right). \quad (4.3)$$

It turns out that the exponential of an anti-Hermitian operator is always unitary, so \hat{U} is always unitary. The exponential of an operator takes the form of the Taylor expansion for complex exponentials.

$$\exp(\hat{O}) = 1 + \hat{O} + \frac{\hat{O}^2}{2!} + \frac{\hat{O}^3}{3!} + \dots \quad (4.4)$$

In the Schrödinger picture we use this unitary operator \hat{U} to evolve the state of the system:

$$|\Psi(t)\rangle = \hat{U}(t)|\Psi(0)\rangle. \quad (4.5)$$

Before we allow our field to interact with the vacuum, we essentially have two closed systems. Thus, *before* interaction we have access to two observables that we can measure: $\hat{a}^\dagger \hat{a}$ and $\hat{b}^\dagger \hat{b}$ - and their real linear combinations. To begin with, this is just measuring the number statistics of $|\psi\rangle$ and the vacuum state. However, as the Hamiltonian acts to evolve the system, we end up with either number detector observing the new, possibly entangled state. Figure 4.1 shows a schematic of what is occurring in the Schrödinger picture.

To simplify analysis, the Heisenberg picture for quantum mechanics shall be employed. As the system evolves over time under the Hermitian Hamiltonian, the operators will evolve

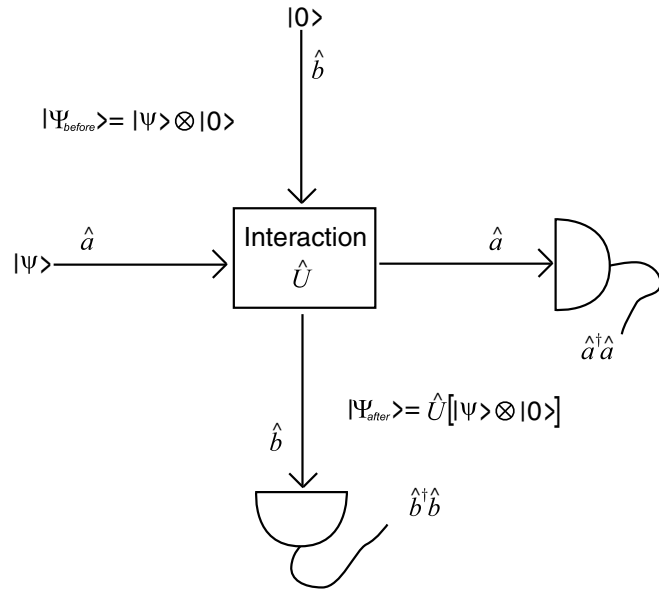


Figure 4.1: A schematic of the system in the Schrödinger picture.

by a unitary operator, $\hat{U}(t)$ say. In fact, if we still assume the system is closed, and we have access to particle counters, then the *only* observables we can measure are precisely the evolved operators of the available observables before interaction. That is, the new evolved operators of $\hat{a}^\dagger \hat{a}$, $\hat{b}^\dagger \hat{b}$ and their real linear combinations. We can find how these operators have evolved in the Heisenberg picture. The unitary operator will act upon the operators in the following way:

$$\hat{O}(t) = \hat{U}^\dagger(t) \hat{O}(0) \hat{U}(t). \tag{4.6}$$

A schematic of the system in the Heisenberg picture is shown in figure 4.2.

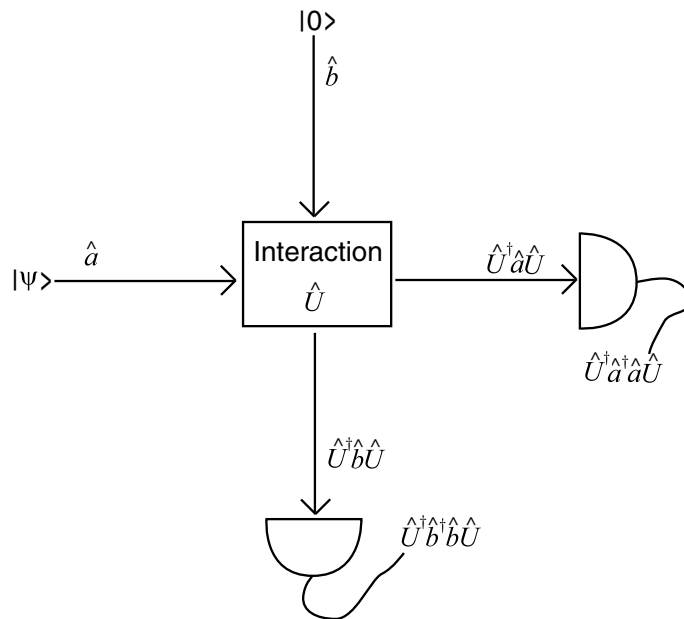


Figure 4.2: A schematic of the system in the Heisenberg picture.

Combining equations 4.2, 4.3 and 4.4 we can see that the form of the unitary operator is restricted. The number of creation minus annihilation operators is zero in each term of the Hamiltonian, and so must also be zero for each term of the unitary operator:

$$\widehat{U}(t) = \sum_{m+n=p+q} d_{mnpq}(t) \hat{a}^{\dagger m} \hat{b}^{\dagger n} \hat{a}^p \hat{b}^q. \quad (4.7)$$

Note that in the previous equation, the field operators are the Schrödinger field operators, that is, the Heisenberg field operators *before* the interaction. This is the convention used for the remainder of this chapter.

As mentioned earlier the operators we can observe begin as $\hat{a}^{\dagger}\hat{a}$ and $\hat{b}^{\dagger}\hat{b}$. In general we can thus observe anything in the following form, or their real linear combinations:

$$\widehat{O}_1 = \widehat{U}^{\dagger}(t)\hat{a}^{\dagger}\hat{a}\widehat{U}(t), \quad (4.8a)$$

$$\widehat{O}_2 = \widehat{U}^{\dagger}(t)\hat{b}^{\dagger}\hat{b}\widehat{U}(t). \quad (4.8b)$$

However, we can see each term of the right hand side is quadratic (same numbers of creation and annihilation operators). Thus, with the most general super-selection Hamiltonian available to us, each term of the allowed observables is quadratic. Furthermore, re-arrangements of such equations can not change this - the only available identities are the commutation relations, which preserve the number of creation minus annihilation operators.

On the Usefulness of Quadratic Observables

The question that next arises is whether or not quadratic observables are useful. Obviously quadratic terms that contain only the \hat{a} operators are simply terms of the form $(\hat{a}^{\dagger}\hat{a})^n$ and, like section 4.1.1, will yield no phase information. Similarly terms involving only \hat{b} operators are not useful.

Thus we must resort to terms involving both operators. The observable we originally set out to obtain was $\hat{a}e^{i\theta} + \hat{a}^{\dagger}e^{-i\theta}$. One might therefore begin to look at quadratic observables such as $\hat{a}\hat{b}^{\dagger} + \hat{b}\hat{a}^{\dagger}$. This I will show contains no phase information in any of its observable moments.

When we measure an observable in a homodyne experiment we see the statistical distribution for that operator. The information in a continuous statistical distribution is stored completely in the moments of that distribution (mean, standard deviation, etc). We can find those moments by the expectation values of the integer powers of the observable in question. That is, for an observable \widehat{O} we can get the statistical information directly from $\langle \widehat{O}^n \rangle$. It is also important to note that the two original states are not entangled - obviously you can not be entangled with the vacuum, or any fully determined sub-state for that matter. Because they are not entangled, we can separate the density matrices, $\hat{\rho} = \hat{\rho}_a \otimes \hat{\rho}_b$. Thus we can also separate their expectation values:

$$\begin{aligned} \langle \hat{a}^{\dagger m} \hat{b}^{\dagger n} \hat{a}^p \hat{b}^q \rangle &= \text{trace} \left[\hat{a}^{\dagger m} \hat{b}^{\dagger n} \hat{a}^p \hat{b}^q \hat{\rho} \right] \\ &= \text{trace} \left[\hat{a}^{\dagger m} \hat{a}^p \hat{\rho}_a \otimes \hat{b}^{\dagger n} \hat{b}^q \hat{\rho}_b \right] \\ &= \text{trace} \left[\hat{a}^{\dagger m} \hat{a}^p \hat{\rho}_a \right] \times \text{trace} \left[\hat{b}^{\dagger n} \hat{b}^q \hat{\rho}_b \right] \\ &= \langle \hat{a}^{\dagger m} \hat{a}^p \rangle \times \langle \hat{b}^{\dagger n} \hat{b}^q \rangle. \end{aligned} \quad (4.9)$$

Everything that is measurable about a quantum operator is given by its statistics. When one prepares a large number of identically prepared systems, and performs a measurement of an observable, given by operator \hat{O} , we can build up a statistical distribution, $p(O)$, say. The expectation values of powers of the observable \hat{O} are related to the moments in the statistics:

$$\langle \hat{O}^n \rangle = \int_{-\infty}^{+\infty} O^n p(O) dO. \quad (4.10)$$

Knowing every one of these expectation values is exactly equivalent to knowing $p(O)$ and thus everything that observable can tell you about the state.

The vacuum state has some interesting properties. In particular, the expectation values of every normally ordered product is zero. This is easy to see from the definition of the vacuum state (equation 2.5).

$$\langle 0 | \hat{b}^{\dagger p} \hat{b}^q | 0 \rangle = 0 \quad (4.11)$$

Furthermore, each non-quadratic term also has zero expectation value, irrespective of ordering. Either equation 2.5 will be evoked when acting on the state, or the inner product after ‘using’ every operator will be between two orthogonal Fock states.

However, not every expectation involving \hat{b} and \hat{b}^\dagger is zero. With a little thought, one can clearly see that anti-normally ordered quadratic terms have non-zero expectation values. Using the definition of the Fock states (equation 2.8c), we arrive at the following result.

$$\langle 0 | \hat{b}^n \hat{b}^{\dagger n} | 0 \rangle = n! \quad (4.12)$$

The expectation value of other orderings can also be determined, with a reasonably obvious algorithm that shall not be stated and is not required in the following.

From these results, we can show that no phase information can be determined about the state we are trying to measure. We have already shown that every observable we can directly measure is quadratic and thus we can write,

$$\hat{O} = \sum_{m+n=p+q} f_{mnpq} \hat{a}^{\dagger m} \hat{b}^{\dagger n} \hat{a}^p \hat{b}^q, \quad (4.13)$$

where we know $f_{mnpq} = f_{pqmn}^*$.

Measuring everything we can with this observable is exactly equivalent to measuring the expectation values of every power of the observable. This will obviously be made up of quadratic terms, and thus can be written in the form:

$$\begin{aligned} \langle \hat{O}^r \rangle &= \sum_{m+n=p+q} g_{rmnpq} \langle \psi | \langle 0 | \hat{a}^{\dagger m} \hat{b}^{\dagger n} \hat{a}^p \hat{b}^q | 0 \rangle | \psi \rangle \\ &= \sum_{m+n=p+q} g_{rmnpq} \langle \psi | \hat{a}^{\dagger m} \hat{a}^p | \psi \rangle \times \langle 0 | \hat{b}^{\dagger n} \hat{b}^q | 0 \rangle, \end{aligned} \quad (4.14)$$

where we also know $g_{rmnpq} = g_{rpqmn}^*$. Using the facts we discovered about the vacuum state, we can simplify this.

$$\langle \hat{O}^r \rangle = \sum_n g_{rn0n0} \langle \psi | \hat{a}^{\dagger n} \hat{a}^n | \psi \rangle \quad (4.15)$$

The only possible information we get about the state is the number information! No

matter which way we manipulate the system or what quadratic operator we end up measuring with, there is no way to get any more information than a simple single detector. Including the vacuum state is thus a completely useless method to find any phase information about the system.

In the Absence of Conservation

I believe it is important to point out that in the absence of super-selection finding the required observable theoretically becomes easy. The displacement operator of section 2.1.2 is a unitary operator that does not conserve particle number. With this operator acting upon the vacuum state we can create a large coherent state useful in Optical Homodyne Tomography (section 3.2.3). The system in figure 4.3 demonstrates the idea.

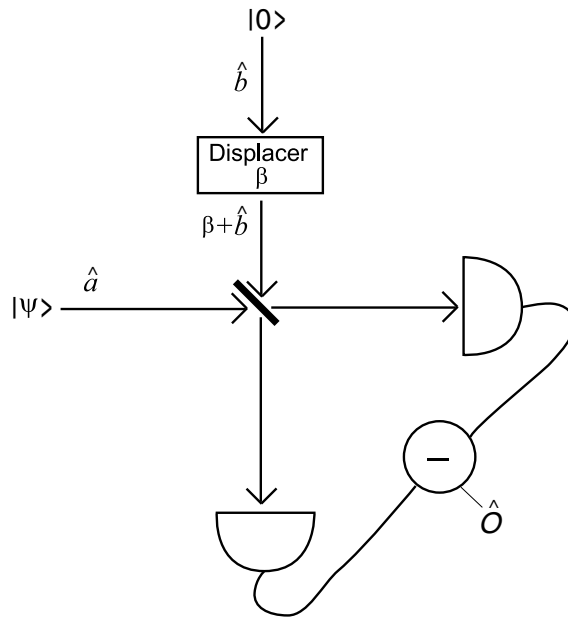


Figure 4.3: The ‘displacer’ can act to create a local oscillator source. This can then be used for standard homodyne experiments.

Using the identity from equation 2.29b and appropriate description for the mirror we can quickly see that the subtracted signal of the two detectors is precisely:

$$\hat{U}^\dagger (\hat{a}^\dagger \hat{a} - \hat{b}^\dagger \hat{b}) \hat{U} = \hat{a}^\dagger (\beta + \hat{b}) + \hat{a} (\beta^* + \hat{b}^\dagger). \quad (4.16)$$

If β is large enough ($\beta \gg \hat{b}$) then this is approximately proportional to the quadrature for \hat{a} .

However, it should be noted that this certainly is not as simple as it seems. When doing an OHT experiment it is necessary to perform the experiment many times to build up statistics (or take many samples of a continuous beam). We require the phase of β to be locked with respect to $|\psi\rangle$ between experiments (or samples), so that the phase statistics don’t “wash out” as the experiment is repeated. In other words, the created coherent state somehow has to have at least classical correlations (or possibly be entangled) with the state we are attempting to measure!

We note that this is easier to achieve in continuous wave experiments. Simply using a well defined ‘clock’ to define our local oscillator, and ensuring that the state $|\psi\rangle$ is a non-

stopping continuous ‘beam’ to represent all elements of the ensemble we wish to measure in the entire experiment, will allow us to create the required classical correlation.

In pulsed experiments, this may be more difficult to achieve. The beginning of each creation of the state $|\psi\rangle$ will need to be locked to the times of our clock, or local oscillator, and the experiments will have to be carried out at fixed time intervals. In particular, for atoms, if we separately ‘created’ two different atomic sources (the local oscillator and the state we are trying to measure), then we would have to phase lock the creation times to each other. The speed of the rotating phase is given by the angular frequency $E = \hbar\omega \approx mc^2$, which is *extremely* fast for atoms (6×10^{24} rad s⁻¹ for ⁴He). We do not have a clock which could be used to accurately begin the two separate apparatus to such precision. However, such a clock could exist if we could coherently ‘create’ the atoms from scratch (see section 3.4).

4.1.3 An Infinite Amount of Nothing

The results of the previous section can be extended for a more realistic situation. A real, single mode BEC is surrounded not by one, but a countably infinite number of other modes. Typically these modes are not empty vacuum in a real BEC experiment - the evaporated atoms are still in the experiment chamber. However, most of these thermal atoms will probably be found in a *thermal* or *chaotic* state (see section 2.1.2). In either the vacuum or the chaotic state, there is no phase information about the state. All the s -parameterised quasi-probability distributions (such as the Wigner, P and Q functions) are radially symmetric about the origin. Now we shall analyse what can be measured in such a system.

States Without Phase

We will now analyse the expectation values of non-quadratic observables on states with no phase information. That is, we can describe the state as a classical mixture of number states. We have already mentioned that such a state will have a radially symmetric Wigner function. This is easy to see. We can find the Wigner function of a classical mixed system by adding the Wigner function of its components weighted with the relevant probabilities:

$$W(\alpha) = \sum_j p_j \times W_j(\alpha). \quad (4.17)$$

The Wigner function of each Fock state is radially symmetric, so the proposed mixture is symmetric. We can create any radially symmetric function as a sum of the Wigner function for Fock states (because Wigner functions of Fock states are given by Laguerre polynomials, which form a complete basis). Since the Wigner function is one-to-one with the density matrix, and therefore fully describes the system, it is the same thing to say the Wigner function is radially symmetric, and the density matrix is diagonal in the Fock basis.

The Wigner function can be used to find the expectation value of any symmetrically ordered operator:

$$\langle : \hat{a}^{\dagger n} \hat{a}^m :_{\text{sym}} \rangle = \iint_{\forall \alpha} \alpha^{*n} \alpha^m W(\alpha) d^2\alpha. \quad (4.18)$$

We can write the Wigner function in polar co-ordinates and separate the variables,

due to the radial symmetry:

$$W(re^{i\theta}) = F(r) \times G(\theta) = F(r). \quad (4.19)$$

The Wigner function is bounded and continuous. It has a finite value at $\alpha = 0$. Then equation 4.18 in polar co-ordinates becomes:

$$\begin{aligned} \langle : \hat{a}^{\dagger n} \hat{a}^m :_{\text{sym}} \rangle &= \int_0^\infty r r^{n+m} F(r) dr \times \int_{-\pi}^\pi e^{i\theta(m-n)} d\theta \\ &= 2\pi \delta_{m,n} \int_0^\infty r^{n+m+1} F(r) dr. \end{aligned} \quad (4.20)$$

It is zero for all $m \neq n$ and thus zero for all non-quadratic terms. This is irrespective of ordering. When one re-arranges an operator into a different ordering (normal to symmetric ordering, say), one uses the commutator for the field operators. This commutator conserves the number of annihilation minus creation operators. Thus when re-arranging a non-quadratic term into symmetric ordering, one creates a sum of non-quadratic, symmetrically ordered terms, all of which have expectation value zero. Thus the expectation value of all non-quadratic operators, in any ordering, for any classical mixture of Fock states, is zero.

This result is a generalisation of one earlier found for the vacuum state. We can use this to generalise the result of equation 4.15.

Systems of Infinite Size

We begin with a system living in an Hilbert space of a countably-infinite number of orthogonal basis states. In one state, with annihilation operator \hat{a} , we have an unknown state that we wish to reconstruct. All other states are labelled with annihilation operators \hat{b}_i for $i \in \mathbb{N}$. These states all have radially symmetric Wigner functions and can be described as a classical mixture of Fock states. We have access to a number of particle detectors (practically, a finite number, but we don't need to assume this).

Before interaction, we have access to any real linear combination of the output of the particle detectors. This observable will be of the form:

$$c_a \hat{a}^\dagger \hat{a} + \sum_{i \in \mathbb{N}} c_i \hat{b}_i^\dagger \hat{b}_i. \quad (4.21)$$

After an interaction between the fields (involving a quadratic Hamiltonian), in the Heisenberg picture we have access to any observable of the form:

$$\hat{O} = c_a \hat{U}^\dagger \hat{a}^\dagger \hat{a} \hat{U} + \sum_{i \in \mathbb{N}} c_i \hat{U}^\dagger \hat{b}_i^\dagger \hat{b}_i \hat{U}, \quad (4.22)$$

where \hat{U} is a quadratic unitary operator, and therefore \hat{O} must also be a quadratic operator.

Following the same line of reasoning as previously, we can conclude no phase information about the state we are interested in can be obtained. Because none of the states are initially entangled with one another, we can apply equation 4.9 component-wise. Any given term of \hat{O}^r contains a finite number of operators. They involve a finite number of \hat{b}_i , where we can index each i as a member of the set $\{p_j\} = \{p_1, p_2 \dots p_J\}$ for some J . With this notation, we then can write down each individual term (of the possible countably

many) of the quadratic operator:

$$\hat{O}^r = \sum_t \hat{T}_t, \quad (4.23)$$

where each quadratic term is in the form:

$$\hat{T}_t = \hat{a}^{\dagger n_a} \hat{a}^{m_a} \times \prod_{i \in \{p_j\}} \hat{b}_i^{\dagger n_i} \hat{b}_i^{m_i}. \quad (4.24)$$

Each operator is separable when taking expectation values:

$$\langle \hat{T}_t \rangle = \langle \hat{a}^{\dagger n_a} \hat{a}^{m_a} \rangle \times \prod_{i \in \{p_j\}} \langle \hat{b}_i^{\dagger n_i} \hat{b}_i^{m_i} \rangle. \quad (4.25)$$

For the term to be non-zero, we require $n_i = m_i$ for each $i \in \{p_j\}$. For the term to be both quadratic and non-zero, we therefore also require $n_a = m_a$. Ignoring each term equal to zero, we then can find:

$$\langle \hat{T}_t \rangle = h_t \langle \hat{a}^{\dagger n_a} \hat{a}^{n_a} \rangle. \quad (4.26)$$

Finally, substituting into equation 4.23, we find the result:

$$\langle \hat{O}^r \rangle = \sum_j k_j \langle \hat{a}^{\dagger j} \hat{a}^j \rangle. \quad (4.27)$$

Again, in this case, the only measurable information about the state is that which could be found by a simple particle counter. We have significantly extended the previous result (equation 4.15) to include an infinite number of participating modes - none of which contain any phase information.

4.1.4 The Requirements of Measurement

We have seen that there exists a strict requirement in order to measure the quantum ‘phase’ statistics of a state. We require the use of a field that contains some phase information. If we allow a quantum state to interact with a state without any phase information, no phase information about the first state can be obtained. Because it is undetectable in any way, in a sense that information contained in the first state has no physical effect at all (on the system). Opening the system up to other states - those containing phase information - may elicit the phase information on the first state.

This brings up a pertinent point about phase in general. It is always true that the physical effects of phase come from relative values between objects. Phase information in a state that exists in a universe of states without any phase information is physically meaningless. A second state to measure relative phase from is required for any physical effect to occur.

Let us take a closer look at the observable $\hat{a} + \hat{a}^\dagger$. We are always allowed to make a global phase shift (or a global change of gauge) in which every (Schrödinger) field operator in the universe is transformed equally. For our field, we can express this as $\hat{a} \rightarrow \hat{a}e^{i\theta}$, and then the quadrature transforms as:

$$\hat{a} + \hat{a}^\dagger \rightarrow \hat{a}e^{i\theta} + \hat{a}^\dagger e^{-i\theta}. \quad (4.28)$$

It appears that changing the gauge also changes the quadrature angle. Although

we are *allowed* to manually set the gauge, and thus define the quadrature properly, the change of gauge should have no physical effect. One might come to the conclusion that the quadrature, as defined above, must also have no physical meaning as it is sensitive to change of gauge. This also appears to apply to all non-quadratic observables.

I would now like to more precisely define what must be meant as measurement, and measurement of a quadrature. If we can only measure quadratic observables (as above), then the previous definition of quadrature is not measurable. Instead, I propose that we *can* write the quadrature as the following, where we require the use of two states, with field operators \hat{a} and \hat{b} , and $\beta \in \mathbb{R}^+$:

$$\hat{X}(\theta) = \lim_{\beta \rightarrow \infty} \frac{\hat{a}^\dagger \hat{b} e^{i\theta} + \hat{a} \hat{b}^\dagger e^{-i\theta}}{\beta}; |\Psi\rangle = |\psi\rangle \otimes |\beta\rangle. \quad (4.29)$$

We note that this is a quadratic observable. To define the quadrature we require the use of a second state. This is consistent with section 4.1.1. Furthermore, we have defined it in terms of a state with the phase defined exactly, and where the amplitude width becomes negligibly small compared to the the absolute amplitude (the use of a coherent state is convenient, but unnecessary). These conditions may also not be met in reality, but we can at least get arbitrarily close to that limit.

However, now we are talking about two modes. To allow all possibilities, we should really be describing the system fully, and not necessarily assume it has no entanglement. A four-dimensional Wigner function should be used to describe the system. Then, the quadrature given above is a marginal (projection) from the four dimensions of the Wigner space to the one-dimensional quadrature axis.

There are different ways for two states to have phase correlations. Previously, we have assumed that they are classical correlations, imposed by the experimenter by the use of a well-defined clock. It would be possible to have quantum entanglement of phase, created for instance by a coherent quantum interaction between modes. The difference between the two situations would be visible in the four-dimensional Wigner function. Simply writing two separated Wigner functions for the two modes, and saying that they have *relative* phase information, does not fully describe all possibilities of the situation.

Currently there is much debate in the field of entanglement in mixed-state systems, and resolution may shed light on what is described here.

4.2 Single Trap BEC

We have seen, that under certain circumstances, there are real, fundamental restrictions on what is measurable about a single mode quantum system of bosons. Up to this point, the discussion has been reasonably abstract. In this section we shall discuss how the previous results relate to dilute-gas Bose-Einstein condensates. Firstly, it is shown that the previous results will also hold for unstable bosons, which is important for real BECs in the lab, such as metastable helium. Secondly, we quickly show that both linear and non-linear BECs can be represented as a countable number of modes of bosons, in order to prove that the previous results can apply to that system.

4.2.1 Unstable Bosons

The super-selection rule imposed to restrict the Hamiltonian to quadratic form implies a conservation of particle number in the system. Earlier, it was mentioned that in some

cases, such as using metastable atoms such as Helium, the particle number in the BEC is not conserved. To conclusively apply the previous section's results to BEC, we would like to cover the case of metastable atoms.

The traditional way of dealing with unstable atoms in BEC theory is one of ignorance of the system. Normally, one does not include the particle loss in the Hamiltonian for the system in question. Through reducing the density matrix of the universe to looking only at the system, one creates a *master equation* to describe the evolution of the reduced density matrix. In this master equation, loss is included, where atoms are lost to the reservoir outside the system. Once lost, all information about the atom is forgotten. Through this method, classical uncertainty in the system is bound to rise, and phase information of the system may become more diffuse. One might therefore assume that no extra information would be obtainable from a system with loss than one without, but we shall prove this more thoroughly.

The atoms that are lost from the system are not lost from the universe. The master equation description is an approximation of reality. A more accurate description is to include the modes that the atom may decay to. Metastable helium, for instance, will often ionise and emit an electron (and another particle, such as a photon, to conserve momentum and energy). This property is exactly why it is easier to create a particle counter for metastable helium than for ground state atoms. Other excited state atoms may simply emit a photon and return to the ground energy state through an electronic rearrangement. If we include the modes of electrons, photons, and other interacting particles, we are still guaranteed to have a Hamiltonian describing the system that has quadratic terms *of the atom number*. This is related to the 'clock problem', discussed in section 3.4. In order to create a non-quadratic Hamiltonian in atom number, we need to have access to energies of the scale of at least the binding energy of the atom. To make it useful, we must be able to coherently control energies of the scale of the atoms' rest mass (section 3.4).

It was mentioned that we allowed quadratic interactions with fermions, such as electrons. In the entire previous section, the mathematics did not require the assumption that the particles are bosons. Of course, Wigner functions and discussion about phase have less meaning for fermions, but mathematically all we assumed was that the form of the commutation relations for the field operators was quadratic (i.e. you can not rearrange the order of field operators in a quadratic equation, and end up with a non-quadratic equation) - which is true for both bosons and fermions.

Thus we can conclude the previous result holds also for unstable bosons. Allowing the ability to detect every mode that the atom could decay to, and each of its products, we still are unable to receive any phase information about the original state.

4.2.2 Measurement of Trapped Dilute-Gas BEC

The results of the previous section hold for a countable, abstract set of bosonic modes, interacting with a quadratic Hamiltonian. We would like to show that we can represent BECs in such a basis. Firstly, we will investigate 'linear' BECs, where each particle is not interacting, and secondly non-linear 'interacting' BECs, where in the semi-classical approximation the BEC does not act in a linear fashion.

Linear BECs

To begin with, we shall look at BECs consisting of particles which do not interact with each other. We assume the BEC is trapped in a quadratic potential. Each individual atom,

then, sees only the potential of a harmonic oscillator. The basis states of the Hamiltonian are those of the harmonic oscillator. A zero-temperature BEC has its population entirely within the ground state. The ground state of a local oscillator happens to have a Gaussian profile, and is a minimum-uncertainty state in position/momentum.

This system consists of one mode of the atom field being occupied by the BEC in question, surrounded by an infinite number of empty spatial modes. We do not have a coherent mode of atoms available to interact with. Thus, interference experiments between atoms can not yield any phase information.

A real BEC will not have zero temperature. A fraction of the BEC, the condensate fraction, will remain in the ground state. The other atoms will occupy different spatial modes of higher energy. The atoms in the linear BEC do not interact with each other what-so-ever. Thus no correlations will be *created* between modes spontaneously. Then, we can see these are purely thermal modes; no phase information can be contained in them. A linear BEC with non-zero temperature also can not yield information about the ground state through atom-interference experiments.

Interacting BECs

An interacting BEC is a very different situation to a non-interacting BEC. A zero temperature BEC will exist entirely in some ground state, interacting or not, and thus we can measure no phase information about it. However BECs never occur without some thermal energy.

Sometimes, interacting BECs are described by the Gross-Pitaevskii equation (also known as the non-linear Schrödinger equation). This leads to a non-linear equation of motion for the BEC. Instead of this approximation, we would prefer to use fully-quantised theory. Here the Hamiltonian is given by the single particle Hamiltonians plus the interaction terms, written with field operators. The following is the Hamiltonian for delta-function interaction potentials, which is usually assumed in BEC modelling:

$$\begin{aligned} \hat{H} &= \int \hat{\psi}^\dagger(\mathbf{r}) \left(-\frac{\hbar^2}{2m} \nabla^2 + V(\mathbf{r}) \right) \hat{\psi}(\mathbf{r}) d^3\mathbf{r} \\ &+ \iint \hat{\psi}^\dagger(\mathbf{r}) \hat{\psi}^\dagger(\mathbf{r}') \left(\frac{U}{2} \delta^{(3)}(\mathbf{r} - \mathbf{r}') \right) \hat{\psi}(\mathbf{r}) \hat{\psi}(\mathbf{r}') d^3\mathbf{r} d^3\mathbf{r}' \end{aligned} \quad (4.30)$$

Note that the above is a quadratic Hamiltonian. We have written the above with respect to the uncountable basis $\{\mathbf{r}\}$. There is absolutely no reason why this Hamiltonian can not be written down with respect to any countable spatial basis ($\{u_n(\mathbf{r})\}$, say), such as the single-particle harmonic oscillator basis mentioned earlier. The system is fully described in a Hilbert space (a countable space), as is always true in quantum mechanics. We can re-write this in a countable basis, where the Hamiltonian becomes:

$$\therefore \hat{H} = \sum_{m,n} (T_{mn} + V_{mn}) \hat{a}_n^\dagger \hat{a}_m + \sum_{mnpq} U_{mnpq} \hat{a}_m^\dagger \hat{a}_n^\dagger \hat{\psi}_p \hat{\psi}_q, \quad (4.31)$$

where:

$$\hat{a}_n = \int u_n^*(\mathbf{r}) \hat{\psi}(\mathbf{r}) d^3\mathbf{r}, \quad (4.32a)$$

$$T_{mn} = -\frac{\hbar^2}{2m} \int u_m^*(\mathbf{r}) \nabla^2 u_n(\mathbf{r}) d^3\mathbf{r}, \quad (4.32b)$$

$$V_{mn} = \int V(\mathbf{r}) u_m^*(\mathbf{r}) u_n(\mathbf{r}) d^3\mathbf{r}, \quad (4.32c)$$

$$U_{mnpq} = \frac{U}{2} \int u_m^*(\mathbf{r}) u_n^*(\mathbf{r}) u_p(\mathbf{r}) u_q(\mathbf{r}) d^3\mathbf{r}. \quad (4.32d)$$

The situation now differs from the linear case in the respect that the different modes may interact with each other (in the linear case, we only have the first sum in equation 4.31, and in the energy eigenstate basis by definition $T_{mn} + V_{mn} = 0$ if $m \neq n$). Although we would not expect the system starting in a chaotic state to evolve into one involving well defined phase correlations, one might expect to see evolution of coherent perturbations of the BEC (the Kerr effect is one example of possible evolution). A partial analysis of perturbations of an interacting BEC in a quasi-particle basis was performed in [17].

Finally, we reach the conclusion that only the number information about the modes of a thermal BEC can be measured. It may be possible to measure correlations between different modes of a perturbed BEC. However, it is not possible to measure the ground state quadrature $\hat{a}_0 + \hat{a}_0^\dagger$ of a BEC.

4.2.3 In Hindsight...

To conclude this chapter we will quickly summarise the above results and some implications to measurement of BEC.

We began by assuming that we do not have access to an absolute phase reference. In section 3.4, we saw that to create one for atoms is not technically feasible. In that section, we saw that we will *never* get phase information about an atomic mode by any interactions with photons. In other words, *no* spectroscopic method would be able to achieve this.

In this chapter it was shown that a super-selective Hamiltonian limits what can be measured about a system. Only observables that are quadratic in atom number can be measured. This has the implication that no absolute phase information is detectable. We can, however, measure quadratic correlations between two different modes. This allows the possibility of using a relative phase reference, but this strictly measures correlations between two modes, and not necessarily any phase information about the two individual states.

The results of this chapter have implications in the field of quantum-atom optics. For instance, Mouritzen and Mølmer produced an interesting paper [17] in which they describe simulation of a BEC and measurements whereby they can partially reconstruct the density operator for the system (see section 3.3.3). Their final claim is that, given the measurement of the ‘anomalous second moment’ of the zero-wave component (i.e. the atoms without momentum), $\langle \hat{a}_0^2 + \hat{a}_0^{\dagger 2} \rangle$, they could detect amplitude squeezing of a state in the Bogoliubov transformation (i.e. a state of quasi-particle excitations). Although this is true, it is clear from this chapter that measurement of the non-quadratic anomalous second moment of atoms may not be possible. Thus, their results agree with this chapter, as they did show that they could not measure amplitude squeezing (which may rely on phase information) without the use of that non-quadratic measurement. Using only the quadratic measurements, they found a difference between a coherent and thermal perturbation. This also agrees as these two states differ in their number statistics.

We have seen that we can only use a relative phase reference. In some cases, we can use large, coherent-like states in order to perform a quadrature ‘measurement’ on the other state (as used in homodyne experiments). This relies on the fact that two states already possess correlations in phase. In these experiments, we are measuring information about

the phase difference between the two states. A good example of this sort of system is that used in OHT and self-homodyne tomography. Typically, the experimenter will begin with a single laser and split into two beams, either spatially (OHT) or in frequency (SHT). There is a set phase correlation between the two sources created by the splitting process, and thus one mode may be used as a relative-phase reference for the other. Note that no experimentalist ever creates and uses an absolute phase reference. To do this we would have to use a laser as a ‘clock’, whereby we could measure the time of *any* event relative to that laser. Such a clock would have resolution of the order of the period of the wave (e.g. 10^{-15} s for optical frequencies), and be able measure times to this accuracy over the total time-scale of the experiment. This is never accomplished in a quantum-optics experiment.

The same is true of BEC. Interference between BECs has been discussed in section 3.3.1. An experimenter could split one BEC into two smaller BECs and expect to see relative-phase information between them. This relative phase information is controlled precisely by the splitting mechanism, and the different conditions that the two condensates endure after splitting. The absolute phase information *before* the splitting is irrelevant in such experiments (however the number statistics may have an effect).

On the other hand, if we create two separate condensates without enforcing correlations, then we will see no relative phase information between the two. Upon interference and measurement, relative phase will be created, but it does not exist beforehand.

Self-Homodyne Tomography for Atom Lasers

In this chapter we deal with inherently multi-mode systems such as the atom laser. We attempt to show that it is possible to adapt self-homodyne tomography for use with atom lasers, by using a relative phase reference. Other correlations may be able to be measured, but are not the focus of the remainder of this thesis. We then analyse some effects caused by poorly defined phase references, which may be a problem in current experiments.

The reason we choose to study self-homodyne tomography is reasonably clear. With lasers, one is easily able to create a phase-locked coherent source to act as the phase reference in optical homodyne tomography (simply by way of a beam splitter). However, with the low atom numbers currently obtainable, this is not feasible for that atom laser. One can make clever use of the atoms already contained in the atom laser to act as the relative phase reference for the experiment by using self-homodyne tomography.

A perfectly single mode (i.e. single momentum) atom laser is experimentally unrealisable. This mode will have infinite spatial extent. In this sense, an atom laser is inherently a multi-mode system. A photon laser also has some finite spread in frequency, and also is a multi-mode field. These devices are useful because they are much *closer* to single-mode operation than classical photon and atom sources. It would be possible to see some interesting correlations between modes in the output of an atom laser, due to the out-coupling process [47].

In addition to the inherent multi-mode characteristic of these fields, we can also impose a multi-mode structure onto these fields. For instance, amplitude- and frequency-modulation has been performed on laser light in order to create frequency side-bands on the laser light field. The separation of the side-bands may be many orders of magnitude smaller than the absolute frequency of the field, and still much larger than the natural linewidth of the beam. This type of side-band creation is also possible with atoms. For instance, Fleischhauer and Gong have proposed a method of transferring side-band squeezing from the photonic to the atomic field [25]. Kheruntsyan and Drummond have suggested using a molecular-BEC to create atom pairs, much like an optical parametric oscillator for photons [43].

5.1 Relative Phase References

It should be recalled that no quantum-optics experimenter uses an absolute phase reference (i.e. a clock accurate to 10^{-15} s). All quantum-optics experiments measure relative phase information. When a coherent state is used to analyse such an experiment, this is an abuse

of notation. However, one finds identical results when one uses the relative coherent state. For instance, if our quantum state consists of only the central frequency and our side-bands, then states with absolute phase would be written as:

$$\hat{\rho} = |\psi(\omega_0 + \Omega)\rangle\langle\alpha_{\omega_0}| |\psi(\omega_0 - \Omega)\rangle\langle\psi(\omega_0 - \Omega)| \langle\alpha_{\omega_0}| \langle\psi(\omega_0 + \Omega)|, \quad (5.1)$$

where the above density matrix can be split into its separate modes, and we can write down well-defined individual Wigner functions for all three frequencies. We can integrate out the absolute phase information to obtain:

$$\hat{\rho} = \int_0^{2\pi} |\psi(\omega_0 + \Omega)e^{i\phi}\rangle\langle\alpha_{\omega_0}e^{i\phi}| |\psi(\omega_0 - \Omega)e^{i\phi}\rangle\langle\psi(\omega_0 - \Omega)e^{i\phi}| \langle\alpha_{\omega_0}e^{i\phi}| \langle\psi(\omega_0 + \Omega)e^{i\phi}| d\phi, \quad (5.2)$$

where I will define the operation on the states $|\psi e^{i\phi}\rangle$ to be equivalent to rotating the individual Wigner function by ϕ . The density operators for this state are not separable. It is important to note that this has *no* effect on any quadratic operator. However, we now satisfy the conditions required in the previous chapter - namely, the state has no absolute phase information.

Throughout this chapter and the next we may write a mode of a bosonic atom field containing absolute phase information. There is no reason to believe that this will lead to results that are any more inaccurate than any obtained in quantum-optics. We can justify this by defining a suitably large state to be the phase reference for the experiment, and always measure phase *relative to it*. It is then a matter of semantics whether you say a second state contains absolute phase information relative to our definition of phase, or relative phase information relative to the first state.

5.2 Side-band Measurement

Given that we are able to create side-band correlations in an atom laser, it would be nice to be able to measure them. In section 3.2.4, we discussed self-homodyne tomography - a method of achieving this for a single spatial mode field. We will now examine the possibility of applying self-homodyne techniques to atom lasers. We will use an analogous experiment to that described in section 3.2.4, in order to find techniques to rotate the quadrature angle.

To achieve this, we will assume that there is a central frequency mode ω_0 , which has a large coherent-like state (i.e. a state of well defined phase¹ and relative amplitude) with amplitude α . The quantum frequency of the atoms corresponds to their (kinetic) energy divided by \hbar , and will depend on the momentum of the atoms. In other words, there exists a coherent state of atoms travelling with some momentum. In addition to this, there may be momentum side-bands (atoms travelling slightly faster and slower than the central, coherent beam). This will, of course, correspond to the frequency side-bands of the atoms, which we will assume for the moment are moving in the same direction as the central beam.

In the photonic case (chapter 3), we wrote the field operator for the frequency mode ω as $\hat{a}(\omega) = \alpha\delta(\omega - \omega_0) + \hat{d}a(\omega)$. However, to be precise, we should avoid this notation. We can assume that the mode at ω_0 has a finite number of atoms in it (in a infinitesimal

¹We mean *relative* phase of *relative* coherent states, such as in equation 5.2.

frequency range), and simply separate the mode by denoting $\hat{a}(\omega) = \hat{a}'(\omega_0)\delta(\omega - \omega_0) + \hat{d}a(\omega)$. Under these conditions, it would make sense to redefine the rotated side-band quadrature operator as:

$$\hat{X}_\Omega(\theta) \equiv \hat{a}(\omega_0 + \Omega)\hat{a}'^\dagger(-\omega_0)e^{-i\theta} + \hat{a}'(\omega_0)\hat{a}^\dagger(\Omega - \omega_0)e^{i\theta}. \quad (5.3)$$

We are now under the same conditions as assumed when we derived the output of a detector, as a function of frequency (equation 3.27), for photons. This equation will hold true for atoms as well, where we are using atomic field operators in place of photonic field operators, and replacing α with $\hat{a}'(\omega_0)$. We found this equation by setting a frequency dependent phase shift on the field operator, equation 3.18:

$$\hat{a}_{\text{out}}(\omega) = F(\omega)\hat{a}_{\text{in}}(\omega).$$

To achieve this for atoms we need to find a way to affect the phase of different modes of the atomic field. This is certainly possible, and is the study of the next chapter. Under the assumption that $|F(\omega)| = 1$, which means the process will not change the mode of the atoms (e.g. the momentum of an atom is the same before and after), we can write:

$$F(\omega) = e^{i\theta(\omega)}, \quad (5.4)$$

and assuming $\omega \neq \omega_0$, we can then re-write the output of a detector as a function of frequency (equation 3.27):

$$\begin{aligned} \hat{O}(\Omega) &= \frac{1}{\sqrt{2\pi}} \left(e^{i(\theta(\omega_0+\Omega)-\theta(\omega_0))} \hat{a}(\omega_0 + \Omega)\hat{a}'^\dagger(-\omega_0) + e^{i(\theta(\omega_0)-\theta(\omega_0-\Omega))} \hat{a}'(\omega_0)\hat{a}^\dagger(\Omega - \omega_0) \right) \\ &= \frac{1}{\sqrt{2\pi}} e^{i\left(\frac{\theta(\omega_0+\Omega)-\theta(\omega_0-\Omega)}{2}\right)} \hat{X}_\Omega \left(\frac{\theta(\omega_0 + \Omega) + \theta(\omega_0 - \Omega) - 2\theta(\omega_0)}{2} \right) \end{aligned} \quad (5.5)$$

Two rotational factors appear in the above. The first term rotates the phase of the frequency output by $(\theta(\omega_0 + \Omega) - \theta(\omega_0 - \Omega))/2$. When performing electronic mixing, this term affects the amplitude of the output, and this factor will have to be taken account of in an experiment. Note that, for small enough Ω , it is approximately equal to the derivative of θ at ω_0 , multiplied by Ω .

More important, however, is the second phase term that modifies the quadrature angle. It is interesting to note, that for small enough Ω , it is approximately half of the second derivative of θ at ω_0 , multiplied by Ω^2 . Manipulation of this value to change quadrature angle is necessary to perform a tomography experiment.

5.3 Limitations Due to Low Atom Numbers

In deriving self-homodyne tomography (section 3.2.4) we have made several assumptions and approximations. In the field of quantum optics, it can be quite easy to achieve the necessary conditions. The large flux of photons in a typical laser beam ($> 10^{15}$ photons per second) make it easy to obtain a state with well defined phase and amplitude. Atomic sources are currently limited to about 10^6 particles per experiment. In this section we shall analyse the effect of relaxing the approximations made earlier on the measurements that are being made.

We are going to use a second state to measure the quadratures, as outlined in section

4.1.4. However, we are not going to assume that we have a large, coherent state to measure with. We wish to see the effect of using any generalised state, described by field operators \hat{b} and \hat{b}^\dagger . In order to be useful in a measurement, it must be a *displaced* state in the sense that we can write:

$$\hat{b} = \beta_0 + \hat{u}, \quad (5.6)$$

where \hat{u} is the operator for a state which has quadrature expectation values of zero:

$$\langle \hat{u} + \hat{u}^\dagger \rangle = \langle i\hat{u} - i\hat{u}^\dagger \rangle = 0. \quad (5.7)$$

One can visualise this state as having a Wigner function which is centred at β_0 , such as in figure 5.1.

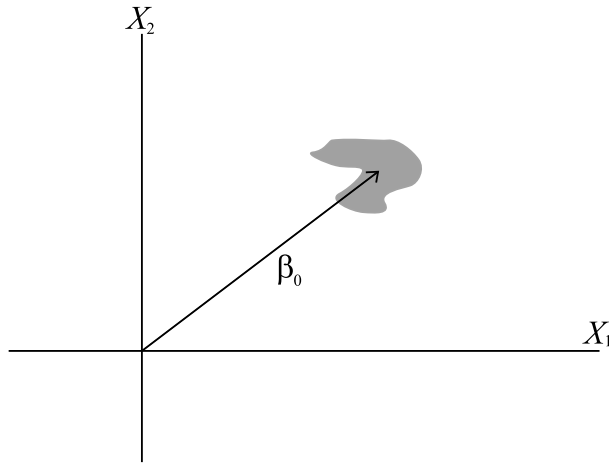


Figure 5.1: The Wigner function of a generalised displaced state, centered at β_0 .

In an experiment with a well-defined phase reference, we would have $\beta_0 \gg \hat{u}$. In this case, we ‘linearise’ the operator by writing $\hat{b} \approx \beta_0$, which is a semi-classical approximation often used in treatments of quantum optics. In the Wigner function picture, such a state appears to be extremely localised around β_0 . Because of the finite width of any Wigner function, this will only happen when $\beta_0 \gg 1$, which requires a large number of particles. For atomic fields of low atom numbers and poor coherences, the linearisation approximation may not hold.

One might note that this seems to be in disagreement with the results of the previous chapter - we can not write down a mode of atoms in a displaced state (because such a state contains phase information on its own). To make this analysis strictly correct, we would require the use of a combined density operator, or the four-dimensional Wigner function for this system. In that picture we *can* define a relative coherent state (as shown in section 5.1). Individually, each state will have no phase information, but together they have correlations which define a relative phase. An analysis which assumes absolute phase information is present is equivalent to assuming that one of the states will be a perfect phase reference for the experiment.

We now will use this state to perform a measurement of the field with annihilation operator \hat{a} . We will measure:

$$\hat{X}(\theta) = \frac{\hat{a}^\dagger \hat{b} e^{i\theta}}{\beta_0} + \frac{\hat{a} \hat{b}^\dagger e^{-i\theta}}{\beta_0^*}. \quad (5.8)$$

If this operator achieved perfect measurement, then it would precisely equal the quadrature $\hat{a}e^{-i\theta} + \hat{a}^\dagger e^{i\theta}$. We shall show that this is not true, because of the finite effect of the operator \hat{u} .

We could rotate the absolute phase of both operators to make $\beta_0 = |\beta_0|$, in which case:

$$\hat{X}(\theta) = \frac{\hat{a}^\dagger \hat{b} e^{i\theta} + \hat{a} \hat{b}^\dagger e^{-i\theta}}{|\beta_0|}. \quad (5.9)$$

Now we will analyse the effect of including \hat{u} on the measurements made. First we must note that this operator, raised to integer powers, does not automatically appear in symmetric ordering (in each separate operator). Thus, we can not interpret this as a marginal of the four-dimensional Wigner function. Because there is no simple way of expressing the probability distribution of the above observable, we shall analyse the first few moments of the distribution.

A quantum statistical distribution is specified by the moments of that distribution (as it is a continuous distribution, for all physically realisable systems). The first moment, $\langle \hat{X}(\theta) \rangle$, corresponds to the mean of the distribution. The second moment, $\langle [\hat{x}(\theta)]^2 \rangle$, is equal to the mean squared plus the variance.

Firstly, we can see that we can precisely predict the first moment of the required quadrature:

$$\begin{aligned} \langle \hat{X}(\theta) \rangle &= \left\langle \frac{\hat{a}^\dagger \hat{b} e^{i\theta} + \hat{a} \hat{b}^\dagger e^{-i\theta}}{|\beta_0|} \right\rangle \\ &= \left\langle \frac{\hat{a}^\dagger (\beta_0 + \hat{u}) e^{i\theta} + \hat{a} (\beta_0 + \hat{u}^\dagger) e^{-i\theta}}{|\beta_0|} \right\rangle \\ &= \langle \hat{a} e^{-i\theta} + \hat{a}^\dagger e^{i\theta} \rangle + \frac{\langle \hat{a}^\dagger \rangle \langle \hat{u} \rangle e^{i\theta} + \langle \hat{a} \rangle \langle \hat{u}^\dagger \rangle e^{-i\theta}}{|\beta_0|} \\ &= \langle \hat{a} e^{-i\theta} + \hat{a}^\dagger e^{i\theta} \rangle. \end{aligned} \quad (5.10)$$

The first moment of our quadratic observable precisely corresponds to what we are trying to measure (the non-quadratic quadrature of \hat{a}). From this measurement, we can determine precisely the centre point of the Wigner function for that state.

As mentioned, the second moment corresponds to the mean (first moment) squared plus the variance. If the second moment was increased, then this corresponds to an increase in the variance of the quadrature observable. The statistical distribution will broaden as ‘noise’ is added to the measurement. We see that a finite width is added to the distribution via the second moment:

$$\begin{aligned} \langle \hat{X}(\theta)^2 \rangle &= \left\langle \left(\frac{\hat{a}^\dagger \hat{b} e^{i\theta} + \hat{a} \hat{b}^\dagger e^{-i\theta}}{|\beta_0|} \right)^2 \right\rangle \\ &= \left\langle \left(\frac{\hat{a}^\dagger (\beta_0 + \hat{u}) e^{i\theta} + \hat{a} (\beta_0 + \hat{u}^\dagger) e^{-i\theta}}{|\beta_0|} \right)^2 \right\rangle \\ &= \langle (\hat{a} e^{-i\theta} + \hat{a}^\dagger e^{i\theta})^2 \rangle + \left\langle \frac{\hat{a}^\dagger \hat{u} \hat{u}^\dagger + \hat{a} \hat{u}^\dagger \hat{a}^\dagger \hat{u}}{|\beta_0|^2} \right\rangle \\ &\quad + \left\langle \frac{\hat{a}^\dagger \hat{a} (\hat{u} e^{i\theta} + \hat{u}^\dagger e^{-i\theta}) + \hat{a} \hat{a}^\dagger (\hat{u} e^{i\theta} + \hat{u}^\dagger e^{-i\theta})}{|\beta_0|} \right\rangle \end{aligned}$$

$$= \langle (\hat{a}e^{-i\theta} + \hat{a}^\dagger e^{i\theta})^2 \rangle + \frac{2\langle \hat{N}_a \rangle \langle \hat{N}_u \rangle + \langle \hat{N}_a \rangle + \langle \hat{N}_u \rangle}{|\beta|^2}, \quad (5.11)$$

where $\hat{N}_a = \hat{a}^\dagger \hat{a}$ is the number operator for the first state and $\hat{N}_u = \hat{u}^\dagger \hat{u}$. \hat{N}_u represents the number of particles *remaining* in the second state *when its Wigner function is displaced to the origin*. In other words, if we applied the displacement operator to the second state so that its Wigner is centred at the origin, then this operator measures the remaining particles in that state.

The last term in the above equation represents the additional variance that is added to the distribution - corresponding to noise on the signal. To achieve a perfect measurement of the quadrature, we would desire this term to approach zero. Therefore, for the measurement to be accurate, we would like to see $|\beta_0|^2 \gg 2\langle \hat{N}_a \rangle \langle \hat{N}_u \rangle + \langle \hat{N}_a \rangle + \langle \hat{N}_u \rangle$.

Recall that a coherent state is simply a displaced vacuum state. In the limit of $\langle \hat{N}_u \rangle = 0$ (which corresponds to a coherent state), then we at least require $|\beta_0|^2 \gg \langle \hat{N}_a \rangle$. In other words, we don't only require a "large coherent state" to measure with, but a "larger coherent state".

The situation gets slightly worse for non-coherent states. It would appear from the above that the coherent state is the perfect state for measurement *for all quadrature angles*. One might imagine using a displaced, squeezed state to measure a particular quadrature more accurately, perhaps at the loss of another, but the above rules out this possibility (as the squeezed vacuum state has finite expectation value of the number operator). It is interesting to note that the phase information of the operator \hat{u} has absolutely no bearing on the outcome of the second moment.

Further moments shall not be analysed, as these moments only affect details of the shape of the distribution, and does not really correspond to noise on the signal.

In equation 5.8 we introduced the quadratic observable used to measure the state of \hat{a} . It is interesting to note the symmetry of this observable. The reason that we can interpret it as measuring something about \hat{a} and not so much about \hat{b} is because of the second state being a large local oscillator. If we do not satisfy the limit $|\beta_0|^2 \gg \langle \hat{N}_a \rangle$, then we can not say that we have this asymmetry. If we write both states as generalised displaced states, then we would find that the outcome of the measurement is a sum of the quadratures from both states, as well as the additional 'noise' just noted.

5.4 Summary

In this chapter, we have shown that it is possible to apply self-homodyne tomography to side-band correlations in atom lasers. In the first section we justify the measurement of relative-phase information, and defend the use of a 'relative coherent state'. We then go on to show that such a 'relative coherent state' can be used perform measurements of correlations between the side-bands, by applying the methods of self-homodyne tomography. Finally, we looked at the potential effects of low atom numbers and poorly defined coherence of the 'relative coherent state'.

In the next chapter we shall provide some concrete examples of methods to perform self-homodyne tomography. The essence of these methods is to create a controllable way to rotate the quadrature angle, so the a full set of quadratures can be measured in order to apply the inverse-Radon transformation.

Proposed Self-Homodyne Techniques For Atom Lasers

The focus of this chapter will be on adapting self-homodyne tomography to find side-band correlations, as defined in section 3.2.4. In the previous chapter, we assumed we were able to make a frequency (energy) dependent phase shift on the mode. In this chapter we suggest several methods of achieving this in an atom laser, focussing on the effects of dispersion in free space and interactions with potentials. A discussion on the effects of gravity is included. Throughout, we analyse the practicality of using the different techniques experimentally.

6.1 Dispersion in Free Space

We now analyse the situation of massive and non-massive bosons in free space, with the hope that evolution of the atom-wave through free space may cause quadrature rotation. Different momentum components of the wave will take different amounts of time to travel, and may arrive at the detector with a relative phase shift - leading to quadrature rotation.

We can write down the field operator as an annihilation of a particle at a given point in space and time $\hat{a}(x, t)$. Alternatively, we can write the field operator in the Fourier domain:

$$\hat{a}(k, \omega) = \frac{1}{\sqrt{2\pi}} \iint e^{i(kx - \omega t)} \hat{a}(x, t) dx dt \quad (6.1)$$

For non-interacting particles, we know that the above wave-number and angular-frequency field operators remain constant (in the Heisenberg picture). In free space, we can write down a simple relationship between ω and k . For instance, photons follow $\omega = kc$ (where c is the speed of light) and non-relativistic atoms will follow $\omega = \hbar k^2/2m$ (where m is the mass of the atom).

The detectors we are using will only measure particles at a point in space and time. Their output is given in terms of Hermitian combinations of the field operators $\hat{a}(x, t)$ and $\hat{a}^\dagger(x, t)$. However, we can connect the output from a point in space to a spectrum analyser, and we may be able to measure $\hat{a}(x, \omega)$. We can determine the behaviour of this operator from the Fourier relations. In this system, we are able to write:

$$\hat{a}(x, \omega) = e^{ik(\omega)x} \hat{a}(0, \omega), \quad (6.2)$$

which is comparable to equation 3.16. Thus, for this system we can write the frequency dependent phase shift $F(\omega) = e^{ik(\omega)x}$. We may experimentally control the position of the detector, at point x . We will now analyse the usefulness of this technique.

6.1.1 Photons

For photons we can write the wave-number as $k = \omega/c$. From this we can see:

$$F(\omega) = e^{i\frac{\omega x}{c}}, \quad (6.3)$$

and can re-write as $F(\omega) = e^{i\theta(\omega)}$, where $\theta(\omega) = \omega x/c$. This is linear in frequency, as we would expect for non-dispersive photons.

The phase rotational term is given as:

$$\frac{\theta(\omega_0 + \Omega) - \theta(\omega_0 - \Omega)}{2} = \frac{\Omega x}{c}, \quad (6.4)$$

but this does not effect the quadrature angle. We actually find that quadrature angle is not changed:

$$\frac{\theta(\omega_0 + \Omega) + \theta(\omega_0 - \Omega) - 2\theta(\omega_0)}{2} = 0 \quad (6.5)$$

This method is not useful for photons in free space. However, it may work for dispersive media. We can write:

$$k = \frac{\omega x}{n(\omega)c} \quad (6.6)$$

For dispersive refractive index n (i.e. one with dependence on frequency), we may be able to rotate the quadrature angle if we can change the thickness of the dispersive material that the light passes through. This may be possible for dispersive, transparent fluids or semi-fluids (such as a human lens). Alternatively, the experimenter could alter $n(\omega)$ of a non-linear medium. Controllable non-linear media with large dispersions are possible, such as those used in EIT (electromagnetically induced transparency) experiments.

6.1.2 Non-Relativistic Atoms

For non-relativistic atoms in zero potential we can write:

$$k = \sqrt{\frac{2m\omega}{\hbar}} \quad (6.7)$$

Note that this is only defined for $\omega \geq 0$. Of course, this is fine as $\hbar\omega$ is the kinetic energy of the particle and is always positive. We have also defined the square root to be positive - the atoms are all travelling in the same direction, which is an accurate assumption.

Given $\theta(\omega) = k(\omega)x$, we can find the rotation of the quadrature for small side-bands (small Ω) as:

$$\begin{aligned} \frac{\theta(\omega_0 + \Omega) + \theta(\omega_0 - \Omega) - 2\theta(\omega_0)}{2} &\approx \frac{1}{2} \frac{\partial^2}{\partial \omega^2} [k(\omega)x]_{\omega_0} \Omega^2 \\ &= \frac{1}{2} \frac{\partial^2}{\partial \omega^2} \left[\sqrt{\frac{2m\omega}{\hbar}} x \right]_{\omega_0} \Omega^2 \\ &= -\frac{x\Omega^2}{4} \sqrt{\frac{m}{2\hbar\omega_0^3}}. \end{aligned} \quad (6.8)$$

Moving the detector (changing x) will change the quadrature angle. Simple dispersion in free space will allow the experimenter to perform a self-homodyne experiment. Note that the zero for x does not necessarily need to be at the atom source. One might mount

the detector on a piezo-electric device for small displacements, or a mechanic device for larger adjustments. Typically the experimenter will need to rotate the quadrature angle by 2π . We can determine how far the detector needs to move in order to perform the experiment. This will depend on the values of Ω and ω_0 . Note that the above is only accurate for small Ω (i.e. $\Omega \ll \omega$). Some numerical results are below.

At first glance, one might think moving the source would be equivalent to moving the detector - and theoretically, this is true. Practically, however, there are complications. If the experimenter tried to move the bottom of a magnetic trap holding a BEC being used as an atom source, then the potential surrounding the atoms may be different. As can be seen in the next section, this may affect the quadrature being measured. If this could be worked around, then the experimenter must be careful that the creation of the atom laser is also unchanged. If the atoms are kicked out of the BEC by a Raman transition, then the Raman lasers will have to be moved with the BEC, possibly affecting the outcome.

6.1.3 Numerical Substitution

Given arbitrary measurement capabilities, this technique will work. We would like to show that it is practical experimentally. We will now calculate some numbers that may apply in metastable helium experiments.

As mentioned earlier, if we want to perform a tomography experiment we will require a full 2π range of quadrature angles to be available. That is, we require equation 6.8 to satisfy:

$$2\pi = -\frac{\Delta x \Omega^2}{4} \sqrt{\frac{m}{2\hbar\omega_0^3}}, \quad (6.9)$$

which we can rearrange to get:

$$\Delta x = \frac{8\pi}{\Omega^2} \sqrt{\frac{2\hbar\omega_0^3}{m}}. \quad (6.10)$$

There will be experimental limitations on the size of Δx . It will not be practical to move the detector by metres, and if Δx is too small then spatial error may be significant.

We will now assume we can create side-bands of any required size. Assuming that the experimenter wants to move the detector by a more reasonable amount, say one millimetre, we can plot the required side-band size versus the central frequency. We will use the units of wave-number (momentum divided by \hbar) for both, as these might be more meaningful to an atom-optics experimenter. The central wave-number k_0 corresponds to the kinetic energy $\hbar\omega_0$. The side-band size Δk gives the difference in momentum of the states with kinetic energy $\hbar(\omega_0 \pm \Omega)$. For $\Delta k \ll k_0$, we have $\Delta k \approx \hbar\omega_0\Omega/m$.

Substituting this into the above and rearranging, we arrive at:

$$\Delta k = 4\sqrt{\frac{\pi k_0}{\Delta x}} \quad (6.11)$$

Note how this simplifies in the wave-number picture. It does not depend on the mass of the boson. The following graph (figure 6.1) of this function will hold for all bosonic atoms, where we have assumed a practical distance that the detector may move ($\Delta x = 1\text{mm}$).

Note that we obviously require $\Delta k < k_0$ (otherwise one side-band would travel in the opposite direction to the central frequency and other side-band). On this graph, that is satisfied for $k_0 > 8 \times 10^5 \text{ m}^{-1}$ (for the case $\Delta x = 1\text{mm}$). For slower atoms, we require more range of movement in the detector. This technique is not practical for atoms that

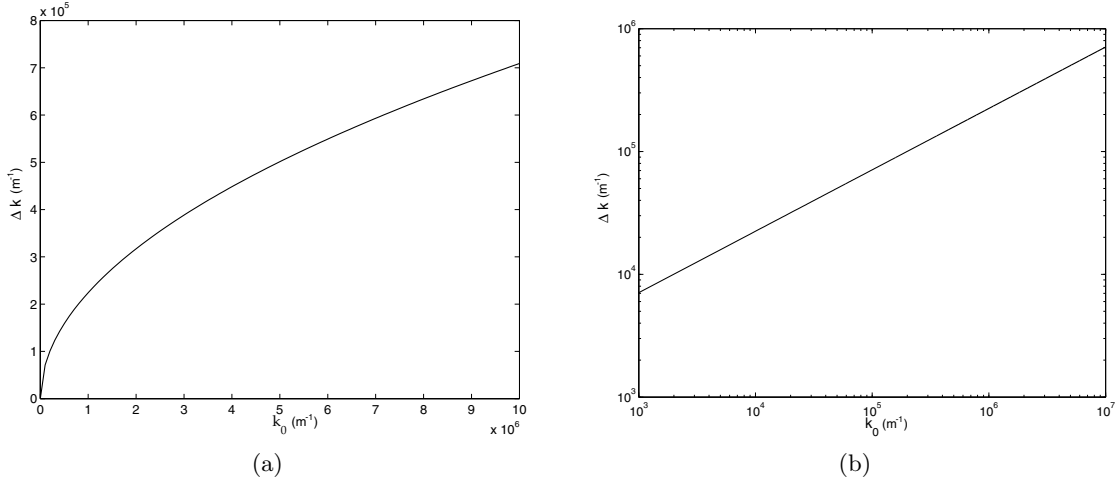


Figure 6.1: We see plotted the required side-band size (in wave-number form) versus the central wave-number, for any bosonic atom, when the experimenter desires to move the detector by 1 mm. This is shown on normal scale (a) and logarithmic scale (b).

move too slow.

It should be pointed out that these results only apply for small side-bands. Earlier, we made a simplification in equation 6.8. The next order term is always of order Ω^2/ω_0^2 smaller. We also assumed this again when converting from frequencies to wave-numbers. If an experimenter is planning on using a system where it is not true that $\Omega^2/\omega_0^2 \ll 1$, then to achieve accurate results the separate terms in equation 6.8 will need to be evaluated and summed, and a non-perturbative conversion between frequency (kinetic energy) and wave-number (momentum) is required.

Transferring Laser Side-bands to an Atom Laser

We will now look at a more concrete example of side-bands on an atom laser. Let us look at the suggestion for side-band creation in atomic beams, where we will create atomic correlations from photonic side-bands [25]. This is achieved by Raman recoil, where an atom will absorb and emit (by stimulation) two near-resonant frequency photons in different directions. The momentum kick to the atom is given by the momentum of the absorbed minus that of the emitted photon, and will depend on the angle of the two beams:

$$\Delta p = \hbar(\mathbf{k}_{abs} - \mathbf{k}_{em}), \quad (6.12a)$$

$$|\Delta p| \leq \hbar(|\mathbf{k}_{abs}| + |\mathbf{k}_{em}|). \quad (6.12b)$$

Let us say that we are using a 1080 nm transition in helium. Given the mass of helium as $m \approx 6.6 \times 10^{-27}$ kg, we can find the maximum velocity as about 1.9 cm/s. This also gives us the kinetic energy, related to the angular frequency:

$$\omega_0 = \frac{p_0^2}{2m\hbar} \approx 1.1 \times 10^6 \text{ rad s}^{-1}. \quad (6.13)$$

We will now follow the method of [25], where we transfer side-band correlations from the optical field to the atomic field. The side-bands are a distance from the central fre-

quency Ω_{photon} . By using modulation techniques, this is currently experimentally realisable in the range of kHz to tens of MHz. The wave-number (momentum) of the side-bands of atoms will be (in the case of perfect laser alignment):

$$k = k_0 \pm \Delta k = k_0 \pm \frac{\Omega_{\text{photon}}}{c}. \quad (6.14)$$

This will give us side-bands in frequency in the atoms, depending on the frequency of the photonic side-bands. For small side-bands, this approximately gives us:

$$\Omega \approx \frac{\hbar k_{\text{photon}} \Omega_{\text{photon}}}{mc} \approx 10^{-3} \text{ to } 10^{-7} \text{ rad s}^{-1}. \quad (6.15)$$

The larger number corresponds to the $\Omega_{\text{photon}} = 10 \text{ Mhz}$, and the smaller 1 kHz. Notice that the side-bands are many orders of magnitude smaller than the total frequency due to the kinetic energy. This is because the side-bands on the photons are also very small.

As mentioned earlier, if we want to perform a tomography experiment we will require a full 2π range of quadrature angles to be available. That is, we require equation 6.8 to satisfy:

$$2\pi = -\frac{\Delta x \Omega^2}{4} \sqrt{\frac{m}{2\hbar\omega_0^3}}, \quad (6.16)$$

which we can rearrange to get:

$$\Delta x = \frac{8\pi}{\Omega^2} \sqrt{\frac{2\hbar\omega_0^3}{m}}. \quad (6.17)$$

For our previous numbers, this would correspond to Δx in the range of 10^{10} to 10^{18} metres! Obviously, under these experimental conditions, it is not possible to perform this experiment. However, by increasing the size of the side-bands, we may be able to get into a realisable regime.

It should be noted that we have analysed a very particular scenario, with small side-bands travelling in the same direction. When creating side-bands on laser beams, it is often much more natural to create side-bands with frequencies as given above, but travelling in different directions. The difference in the wave-vectors between the side-bands will be quite large, even though they have approximately the same frequency. When the side-bands are transferred to atoms, the projection of the momentum of the side-bands in a given direction will be much larger than the numbers given above. It should be reasonably easy to create momentum side-bands that are of a comparable size (maybe a factor of 10 to 100 times smaller) to the total momentum using this method. We would then be able to move the detector many orders of magnitude less distance to get a 2π quadrature rotation. However, using this technique, the resulting atoms will be travelling in different directions. If the change in direction is small enough, we may be able to ignore this. An analysis of multi-dimensional motion, such as this, may be the subject of future work.

It should also be pointed out that the above results are specifically for the case of small side-bands ($\Omega \ll \omega_0$). For larger side-bands, it is a necessary (but simple) task to evaluate the individual terms on the left-hand-side of equation 6.8.

6.2 Using Potential to Control Quadrature Angle

Moving the detector may not be a feasible method of detection for all experiments. We can change the potential that the atoms are subject to in order to change the quadrature

angle. We will apply the WKB approximation [45] to approximately find the evolution of the field operators in a slowly varying field. The WKB approximation is most valid in situations without classical turning points (potential becoming greater than the total energy) or much reflection (caused by the potential changing rapidly over scales of the inverse wave-number, or wavelength).

Physically, the WKB approximation is similar to the adiabatic approximation. In the adiabatic approximation, one changes the potential in time slowly and, if it is slow enough, the state will coherently evolve with it. A state in the ground state will remain in the ground state. In the WKB picture, a travelling wave encounters a slowly changing potential. A ‘travelling point’ in the wave will only ‘notice’ a slow change in potential. The wave coherently ‘follows’ the potential in the sense that it keeps travelling in the same direction and conserves its energy. The wave-vector (momentum) for that part of the wave will change as some kinetic energy is converted to potential energy.

6.2.1 Simple Potential

We now wish to analyse the effect of small changes of potential to non-relativistic atoms, and possible methods to control quadrature angle. We will begin with a simple system to analyse - a one-dimensional system, where the source and detector have in-between a region of length x , with potential raised by ΔU , as depicted in figure 6.2. More complicated potentials (including gravity) will be dealt with later.

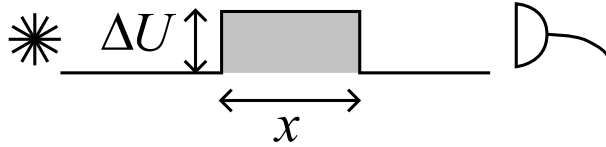


Figure 6.2: A controllable ‘top-hat’ potential sits between the atom source and the detector.

The wave will travel through this region and ‘slow down’. The amplitude will also increase in this region, and decrease to the same as before after it passes through the other side. The WKB approximation will hold if there is little reflection - that is, the change in potential energy is small compared to the total kinetic energy:

$$\Delta U \ll \frac{\hbar^2 k^2}{2m}. \quad (6.18)$$

In the WKB approximation, we know that:

$$\hbar\omega = \frac{\hbar^2 k(x)^2}{2m} + U(x), \quad (6.19)$$

and given energy conservation we know ω is a constant. The wave-number in the increased potential is:

$$k = \sqrt{\frac{2m}{\hbar} \left(\omega - \frac{\Delta U}{\hbar} \right)}. \quad (6.20)$$

The phase shift on the wave through the raised potential region is the same as equation

6.2. Thus, we can see that the field operators undergo a phase shift:

$$\theta(\omega) = kx = \sqrt{\frac{2m}{\hbar} \left(\omega - \frac{\Delta U}{\hbar} \right)} \times x \quad (6.21)$$

Following a similar method to the previous section, we find that the rotation to the quadrature angle is given as:

$$\begin{aligned} \frac{\theta(\omega_0 + \Omega) + \theta(\omega_0 - \Omega) - 2\theta(\omega_0)}{2} &\approx \frac{1}{2} \frac{\partial^2}{\partial \omega^2} \left[k(\omega)x \right]_{\omega_0} \Omega^2 \\ &= -\frac{\Omega^2 x}{4 \left(\omega_0 - \frac{\Delta U}{\hbar} \right)^{3/2}} \sqrt{\frac{m}{2\hbar}}, \end{aligned} \quad (6.22)$$

where we have assumed that the side-bands are small compared to the central mode.

We must note that the rotation is not zero for $\Delta U = 0$. This is similar to the detector-moving case where the rotation is never zero for a detector a finite distance away, but all the experimenter is interested in is any 2π range of rotation angles. The rotation difference between $\Delta U = 0$ and a finite value is given by:

$$\Delta\phi(\Delta U) = \frac{\Omega^2 x}{4} \sqrt{\frac{m}{2\hbar}} \left[\frac{1}{\omega_0^{3/2}} - \frac{1}{\left(\omega_0 - \frac{\Delta U}{\hbar} \right)^{3/2}} \right] \quad (6.23)$$

In the same limit that the WKB approximation holds (equation 6.18), we can also invoke the binomial approximation to the previous equation (as the kinetic energy roughly equals $\hbar\omega_0$). For an experimenter to be able to perform a tomography experiment, a full 2π range of quadrature angles will have to be available. If we begin with zero potential and raise it to ΔU , then we need to satisfy:

$$2\pi = \frac{3\Omega^2 x \Delta U}{8\hbar\omega_0^{5/2}} \sqrt{\frac{m}{2\hbar}}. \quad (6.24)$$

We can plot values of $\Delta U \times x$ for ^4He . These results will be true for all values of the product, but we must note that it *only* holds true when $\Delta U \ll \hbar\omega_0$. There was also the original approximation that the side-band size was small. In figure 6.3, we plot this in terms of wave-numbers:

$$\Delta U \times x = \frac{8\pi\hbar^2 k_0^3}{3m \Delta k} \quad (6.25)$$

It should be pointed out that in a region of this plot $\Delta k > k_0$. Obviously this situation would not be allowed, as one of the side-bands would be travelling in the opposite direction to the rest of the atoms! It also breaks the previous assumption about small side-bands. The upper-left triangular region of this graph is most accurate.

The experimenter will need to make sure that $\Delta U \ll \hbar^2 k_0^2 / 2m$ (for the top hat potential to appear approximately smooth), and may also wish to minimise x (compared to, say, the results of the previous section, where we found the detector had to move 10^9 metres). From this graph, we can see that larger Δk will result in a smaller product $\Delta U \times x$. It is probable that tiny side-bands (such as those created by the method of [25] where the beams travel in the same direction) will not be detectable in this scheme either.

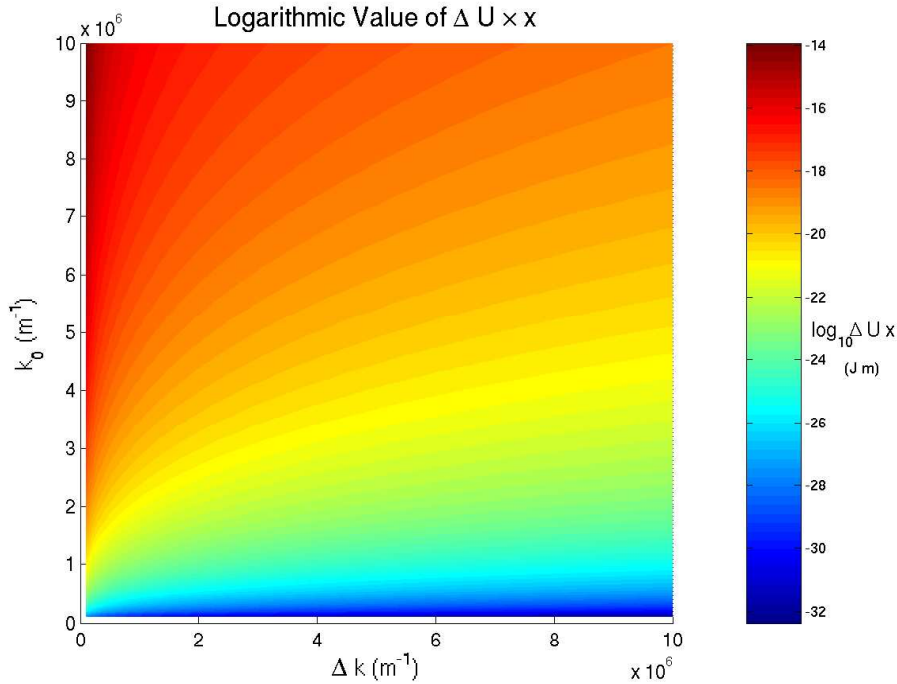


Figure 6.3: We see plotted the required size of $\Delta U \times x$ versus the side-band size (in wave-number form) and the central wave-number, for helium-4, when the experimenter desires to rotate the quadrature using the potential.

6.2.2 General Potentials

Experimental production of ‘top-hat’ style potentials for atoms would be extremely difficult. Luckily, the WKB approximation is simple to apply to potentials of any shape. Indeed, it would be more accurate for smooth potentials. To simplify analysis, we will allow any shape potential between two points x_1 and x_2 , where the potential is constant and equal on either side of the ‘barrier’. This is depicted in figure 6.4.

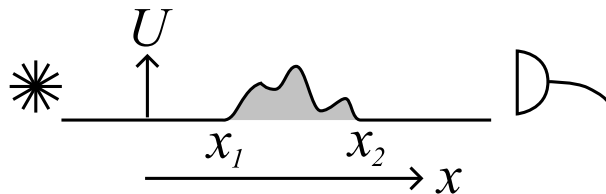


Figure 6.4: A controllable potential of any shape sits between the atom source and the detector.

The WKB approximation will apply easily to this situation. In this case we will sum up (integrate) the *differential phase shifts* over a length. The phase shift over a small distance dx is given by $k(x) \times dx$. We note that $k(x)$ will depend upon the energy of the wave, so we write $k(x, \omega)$. The total phase shift over the region is given by:

$$\theta(\omega) = \int_{x_1}^{x_2} k(x, \omega) dx. \quad (6.26)$$

We then apply the same method as previously (assuming relatively small side-bands),

to get a quadrature rotation of:

$$\frac{\theta(\omega_0 + \Omega) + \theta(\omega_0 - \Omega) - 2\theta(\omega_0)}{2} \approx \frac{-\Omega^2 x}{4} \sqrt{\frac{m}{2\hbar}} \int_{x_1}^{x_2} \frac{1}{\left(\omega_0 - \frac{U(x)}{\hbar}\right)^{3/2}} - \frac{1}{\omega_0^{3/2}} dx. \quad (6.27)$$

If the kinetic energy is not significantly altered (even in a smooth manner) then we can apply the binomial approximation, to find the amount of quadrature rotation, $\Delta\phi$, compared to the case $U(x) = 0$:

$$\Delta\phi \approx \frac{3\Omega^2}{8\hbar\omega_0^{5/2}} \sqrt{\frac{m}{2\hbar}} \int_{x_1}^{x_2} U(x) dx. \quad (6.28)$$

We see this is proportional to the ‘area’ of the energy - depicted as the grey shaded area in figure 6.4. This equation is the same as equation 6.24 with the shaded area given in figure 6.2. If the experimenter desires a 2π range in this angle, then we can re-interpret the previous numerical results as being plotted against the integrated potential ‘area’.

The experimenter may run into the problem given in the previous section, where we require a large distance $x_2 - x_1$ in order to rotate the quadrature significantly. This may be necessary in order to satisfy the assumption $U(x) \ll \hbar\omega_0$. This assumption is not necessary. If one wishes to see a large change in quadrature angle over a short distance, then it may be practical to smoothly alter the kinetic energy *significantly*. When the particles are slowed down to a fraction of their previous speed, then the side-bands and central frequency will be moving at relatively different velocities. In that case, the approximated results will not hold, and the integral in equation 6.27 will have to be evaluated. This should be a reasonably simple task once the shape of the potential is known. It is suspected that an experimenter will have to push this technique to its limits, by using a large, smooth change in potential. However, at these limits, the experimental uncertainty in potential may pose significant difficulties. This may be the subject of future work.

6.3 Gravity

As yet, we have not discussed the effects of gravity. Gravitational forces may be very important to the motion of an atom laser. Indeed, in some experimental set-ups, atoms are slowly ‘released’ from the BEC and fall vertically under the influence of gravity. In these cases, we can easily determine the dynamics of the atom laser. What is unclear is the effect it will have on a quadrature measurement. When an atom laser has a horizontal momentum component, then the path will bend in a parabola. Different momentum components of the beam will separate both horizontally and vertically. We shall analyse the effect of these two cases now.

6.3.1 Vertical Motion

Imagine an atomic BEC sitting in a trap at some height h above a detector. Atoms are released from the trap with some (downward) vertical momentum $\hbar k$. They begin with kinetic energy $\hbar\omega = \hbar^2 k^2 / 2m$. The set-up is shown in figure 6.5.

The potential as a function of distance below the trap, z , is $U(z) = -mgz$. This is a one-dimensional problem, where the potential is smooth (when the velocity is not extremely small) and we can apply the WKB approximation to the evolution of the wave.

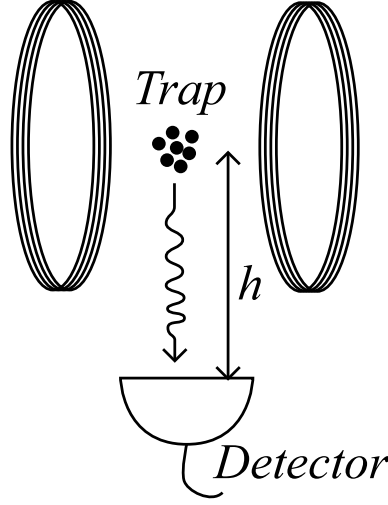


Figure 6.5: The atoms sit in a trap and are slowly released. The wavelength of the atoms decrease as they accelerate downwards, toward the detector.

We can use energy conservation to find the wave-number as a function of height:

$$k(z) = \sqrt{\frac{2m}{\hbar} \left(\omega + \frac{mgz}{\hbar} \right)}. \quad (6.29)$$

We can integrate this to find the total phase change at the detector:

$$\begin{aligned} \theta(\omega) &= \int_0^h k(z) dz = \int_0^h \sqrt{\frac{2m}{\hbar} \left(\omega + \frac{mgz}{\hbar} \right)} dz \\ &= \frac{2}{3} \sqrt{\frac{2\hbar}{mg^2}} \left[\left(\omega + \frac{mgh}{\hbar} \right)^{3/2} + \omega^{3/2} \right]. \end{aligned} \quad (6.30)$$

Note that this time the potential at the source is not equal to that at the detector. This will have an effect on the amplitude of the wave. WKB theory can correctly predict the amplitude of the wave. The change of amplitude will act to conserve the *flux* of atoms in the beam - all points in z should expect to see the same number of atoms pass in a given time (on average). This will have a simple effect on the field operators, but we shall not analyse it here.

Assuming that we have a side-band type of output, centred at ω_0 , we can apply the previous results to find the quadrature rotation.

$$\Delta\phi = \frac{\theta(\omega_0 + \Omega) + \theta(\omega_0 - \Omega) - 2\theta(\omega_0)}{2} \approx \frac{\Omega^2}{12g} \sqrt{\frac{2\hbar}{m}} \left[\frac{1}{\sqrt{\omega_0}} - \frac{1}{\sqrt{\omega_0 + \frac{mgh}{\hbar}}} \right] \quad (6.31)$$

The quadrature will rotate as it drops. An experimenter could, as before, move the detector between ‘shots’ and perform a tomography experiment. The question remains, what is the effect on the distance the experimenter needs to move the detector? Is it greater or smaller?

To quantify the rate that the quadrature changes, we can simply take the derivative as a function of height h .

$$\frac{\partial \Delta \phi}{\partial h} = \frac{\Omega^2}{4 \left(\omega_0 + \frac{mgh}{\hbar} \right)^{3/2}} \sqrt{\frac{m}{2\hbar}} \quad (6.32)$$

This quantity represents the rate of change of quadrature angle with respect to (vertical) movement of the detector. This is height dependent. Integrating this function between two points gives the amount the quadrature has rotated in that distance.

We can also find the rate of change of quadrature rotation with respect to detector movement for the horizontal case, equation 6.8. In that case we have:

$$\frac{\partial \Delta \phi}{\partial x} = \frac{\Omega^2}{4\omega_0^{3/2}} \sqrt{\frac{m}{2\hbar}} \quad (6.33)$$

The ratio of these two quantities represents the ratio of the quadrature rotation over a small distance. Dividing equation 6.32 by equation 6.33 we arrive at the quantity:

$$\frac{1}{\left(1 + \frac{mgh}{\hbar\omega_0} \right)^{\frac{3}{2}}} \quad (6.34)$$

This ratio is smaller than unity. This means the rate of quadrature rotation (with respect to detector movement) *decreases* when the atoms are sped up under gravity. That is, the distance the detector needs to move *increases*. This may be useful to the experimenter if it easier to move the detector by a larger distance.

To achieve the opposite effect, one could ‘kick’ the atoms vertically up. The atoms will slow down as they approach the detector, and we will see the opposite effect to falling. Mathematically, this is precisely equivalent to making h negative. Doing this may be useful if the experimenter wants to reduce the distance the detector must travel, for instance, because of limited space in the experimental chamber. One must note that the turning point can not be exceeded (the turning point is when equation 6.34 goes infinite), or the atoms will not hit the detector. Also, this implementation of the WKB approximation will break down very close the turning point.

Numerical Analysis of Gravitational Effects

We have just pointed out that we can use gravity to either increase or decrease the distance a detector needs to move in a dispersion tomography experiment. Given this ultimate control, one might imagine using this to measure side-bands of any separation, on a beam starting with any momentum. This is not practical, however.

Let us examine the situation mention in section 6.1.3. We begin with helium-4 being Raman kicked with two beams of wavelength 1080 nm. Let us first imagine that atoms began to travel downwards. It would probably be improbable that the experimentalist could get the detector closer than one millimetre to the source (typically a BEC). Under these conditions, we have $mgh/\hbar\omega_0 \approx 0.57$, and we can evaluate equation 6.34 and get a ratio of 0.51. In other words, if we move the detector by a small distance, we receive approximately half the quadrature rotation than the case without gravity. If the detector is an entire centimetre away, then this ratio reduces to approximately 0.058. The detector will have to move about seventeen times further in order to acquire the same quadrature rotation. At ten centimetres, the ratio is closer to 2.2×10^{-3} , where the detector will need to move a factor of around 450 times further. Much larger distances will not be practical

in an experimental chamber.

On the other hand, we may wish to reduce the distance the detector can move. This will be necessary for very small side-bands. For a simple Raman kick, we found we only received a velocity of about 1.9 cm/s. If this is directed vertically, then the turning point will be a distance of 2×10^{-5} m, or twenty micron, above the source. It would be completely impractical to place a detector this close to a BEC. Therefore, we can rule out this possibility for atom lasers that receive their momentum via a Raman transition. It may be useful for other atom-laser creation methods that can generate faster velocities.

6.3.2 Two-Dimensional Motion

We saw earlier that the Raman ‘kick’ to the helium atoms produced a velocity of a few centimetres a second. Obviously gravity would play an important role in the motion of the particles. If this was to be a horizontal kick, then the motion would stay approximately straight for only a few hundredths of a millimetre. After this, acceleration due to gravity will have given a significant vertical component to the velocity, and it would follow the usual parabolic trajectory.

Gravity will severely complicate the motion. In particular, different momentum components of the wave may begin to separate as they follow different parabolic trajectories. This may actually be useful if one desires to separate well-defined side-bands (i.e. side-bands with small width that are separated significantly from the central frequency). In essence, one would be taking different momentum modes in the same spatial mode, and separating them into different spatial modes. Once in different spatial modes, they could be manipulated separately quite easily. This would allow a whole range of different interference-type experiments to be achieved (such as homodyne and heterodyne experiments). We would not necessarily have to perform self-homodyne measurements. Other observables may be easily accessible, such as two-mode correlations $\hat{a}\hat{b}^\dagger + \hat{a}^\dagger\hat{b}$ (note that one would not have to separate spatial modes in order to measure this either).

A more thorough analysis of two dimensional motion may be the subject of future work.

Conclusions

In this thesis we have presented a theoretical investigation into the possibility of performing quantum state reconstruction on ultra-cold atomic sources.

It was found that, due to super-selection rules acting to conserve the number of atoms, it is only possible to measure observables that are quadratic in the atom field operators. We have formally shown that, if a system begins with no absolute phase information, then no absolute phase information can be obtained what-so-ever. Therefore, it is not possible to create a coherent state of atoms, or indeed any state containing absolute phase information (i.e. absolute relative to a classical clock). We come to the conclusion that it is impossible to perform a measurement of the single-mode quadrature (e.g. $\hat{a} + \hat{a}^\dagger$). In fact, because it is theoretically not measurable in any way, the phase information contained in this operator can have no physical effect. If a single mode is surrounded by states lacking absolute phase information, only the number statistics of that mode has physical meaning.

However, we can still perform measurements of quadratic correlations between different states. Examples of operators that represent such correlations include $\hat{a}^\dagger \hat{b} + \hat{a} \hat{b}^\dagger$. Furthermore, we are allowed to have states with relative phase information, which can be measured with quadratic observables. This allows the possibility of writing down a ‘relative coherent state’, a mode of the field with well defined phase relative to some other modes. This state does not, however, contain phase defined with respect to atomic modes with which it has not interacted.

We then went on to find methods of measuring such observables, in the hope of performing quantum state reconstruction of correlations in atomic sources. We showed that this was possible for side-band correlations in atom lasers, by adapting a method known as self-homodyne tomography traditionally used in the field of quantum optics. Other quantum-optics methods would be less useful due to the difficulty in creating a separate beam with defined relative phase. The usefulness of this technique relies on there being well defined phase relationships between the modes of the field. It is more difficult to create a well defined phase for atoms (than photons) because of the low particle number. We have analysed the effects of a poorly defined relative phase reference on self-homodyne techniques. We found that the best phase reference is always a coherent state, independent of quadrature angle. All that remains to perform such an experiment is a way of rotating the quadrature angle, in order to use tomography to reconstruct the state.

Several experimental methods of performing the necessary quadrature rotations have been proposed. The first method takes advantage of dispersion in free space for massive bosons. Simply moving the location of the detector will rotate the quadrature measured. We also found that changing the potential that the atoms travel through will alter the measured quadrature angle. Limitations on the separation of the side-bands were found with these methods. In particular, measuring side-bands with extremely small separation

is not practical.

Finally, the gravitational potential was considered. We found that gravity will affect the distance a detector is required to move (in the first method mentioned in the previous paragraph). The detector will need to move a greater distance for accelerated atoms, and a lesser distance for atoms which have been slowed by gravity. We analysed this numerically for the case of helium-4 undergoing a Raman transition at 1080 nm, and saw that it is not practical to aim the atoms upward to decelerate via gravity.

Directions for Future Work

Theoretical analysis of these techniques is far from complete. Further work would be required before experimentation could begin. Some directions for future work would include:

- Finding accurate limits of these methods in experimental design. Of particular importance is finding the limits on bandwidth (i.e. the side-band separation). There are several parameters with experimental constraints and uncertainty that will limit this band-width. We have already seen that the detector-moving method will not be practical for tiny bandwidths due to the limitations on the amount the detector can move. Other practical limitations may include: position uncertainty, uncertainty in the potential, and detector efficiency.
- A thorough investigation of two- and three-dimensional motion. The beams are likely to diffuse in the directions perpendicular to the main travel, which will complicate analysis. We have seen gravity plays a major role in the motion of the beams. Experiments involving multiple spatial modes may be useful and necessary. It might be possible to remove the other dimensions from the problem by applying a wave-guide to the atoms (e.g. by allowing them to travel in the direction of a ‘red-detuned’ laser beam that is creating an attractive, cylindrically symmetric potential).
- Investigating the ‘natural’ side-band correlations that occur in the out-coupling procedure. It has been suggested [47] that correlations between momentum modes will exist after out-coupling. These will be correlations between modes inside a relatively wide ‘envelope’, which may require slightly different analysis to the types of side-band correlations discussed in this thesis (i.e. those with a large, central mode).

Bibliography

- [1] S. N. Bose, “Z. Phys. **26**, 178”, 1924
- [2] A. Einstein, “Sitzungsberichte der Preussischen Akademie der Wissenschaften Physikalisch-mathematische Klasse”, 1924 (p. 261), 1925 (p. 3)
- [3] F. London, “Nature **141**, 643”, 1938; “Phys. Rev. **54**, 947”, 1938
- [4] M. H. Anderson, J. R. Ensher, M. R. Matthews, C. E. Wieman, and E. A. Cornell, “Science **269**, 198-201”, 1995
- [5] K. B. Davis, M. O. Mewes, M. R. Andrews, N. J. Van Druten, D. S. Durfee, D. M. Kurn, and W. Ketterle, “Phys. Rev. Lett. **75**, 3969”, 1995
- [6] C. C. Bradley, C. A. Sackett, J. J. Tollet, and R. G. Hulet, “Phys. Rev. Lett **75**, 1687”, 1995
- [7] A. Robert, O. Sirjean, A. Browaeys, J. Poupard, S. Nowak, D. Boiron, C. I. Westbrook, and A. Aspect, “Science, 292:461”, 2001
- [8] F. Pereria Dos Santos, J. Leonard, J. Want, C. J. Barrelet, F. Perales, E. Rasel, C. S. Unnikrishnan, M. Leduc, and C. Cohen-Tannoudji “Phys. Rev. Lett., **86**(16):3459-3462”, 2001
- [9] T. M. Hanna, Honours Thesis: “*Loading of a magneto-optical trap of metastable helium*”, The Australian National University, 2003
- [10] J. Bertrand and P. Bertrand, “Foundations of Physics **17**, 397”, 1987
- [11] K. Vogel and H. Risken, “Phys. Rev. A **40**, 2847”, 1989
- [12] G. M. D’Ariano, C. Macchiavello and M. G. A. Paris, “Phys. Rev. A **50**, 4298”, 1994
- [13] E. T. Jaynes, “Phys. Rev. **108**, 2, 171”, 1957
- [14] V. Bužek and G. Drobný, “Journal of Modern Optics, **47**, no 14/15, 28232839”, 2000
- [15] G. Drobný and V. Bužek, “*Reconstruction of motional states of neutral atoms via the **MaxEnt** principle*”, arXiv:quant-ph/0202080 v1, 2002
- [16] E Skovsen, H. Stapelfeldt, S. Juhl and K. Mølmer, “Phys. Rev. Lett. **92**, 090406”, 2003
- [17] A. S. Mourtizen and K. Mølmer, “*Tomographic reconstruction of quantum correlations in excited Bose-Einstein condensates*”, arXiv:cond-mat/0409500, 20 Sep. 2004
- [18] D. T. Smithey, M. Beck, J. Cooper, and M. G. Raymer, “Phys. Rev. Lett. **70**, 1244”, 1993

-
- [19] D. T. Smithey, M. Beck, J. Cooper, M. G. Raymer, and A. Faridani, “Phys. Scr. **T48**, 35”, 1993
- [20] D. T. Smithey, M. Beck, J. Cooper, and M. G. Raymer, “Phys. Rev. A. **48**, 3159”, 1993
- [21] C. Kurtsiefer, T. Pfau, and J. Mlynek, “Nature **386**, 150”, 1997
- [22] M. D. Levenson, R. M. Shelly, and S. H. Perimutter, “Optics Letters **10**:10, p814”, 1985
- [23] P. Galatola, L. Lugiato, M. Porreca, P. Tombesi, and G. Leuchs, “Opt. Commun. **85**, 95”, 1991
- [24] A. Zavatta, F. Martin, G. Giacomelli, “Phys. Rev. A **66** 043805”, 2002
- [25] M. Fleischhauer and S. Gong, “Phys. Rev. Lett. **88**, 070404”, 2002
- [26] Jinwei Wu, PhD Thesis: “*Applications of Optical Homodyne Tomography*”, The Australian National University, 1999
- [27] E. P. Wigner, “Phys. Rev. **40**, 749”, 1932
- [28] K. E. Cahill and R. J. Glauber, “Phys. Rev **177**, 1882”, 1968
- [29] Y. Castin and J. Dalibard, “Phys. Rev. A **55**, 4430”, 1997
- [30] J. I. Cirac, C.W. Gardiner, M. Naraschewski and P. Zoller, http://www.vuw.ac.nz/staff/crispin_gardiner/BEC/960531lastv.pdf, Viewed 1/10/2004
- [31] J. I. Cirac, C. W. Gardiner, M. Narachewski and P. Zoller, “Phys. Rev. A, **54**(5) 3714”, 1996
- [32] P. Horak and S. M. Barnett, “J. Phys. B **32**, 3421”, 1999
- [33] R. Graham, T. Wong, M. J. Collett, S. M. Tan and D. F Walls, “Phys. Rev. A **57**, 493”, 1998
- [34] J. A. Dunningham, “Phys. Rev. A **66**, 041601(R), 2002
- [35] D. C. Roberts and K. Burnett, “Phys. Rev. Lett. **90**, 150401”, 2003
- [36] T. Wong, M. J. Collett and D. F. Walls, “Phys. Rev. A **54**(5), R3718”, 1996
- [37] E. M. Wright, T. Wong, M. J. Collett, S. M. Tan and D. F. Walls, “Phys. Rev. A **56**, 519”, 1997
- [38] A. Sinatra and Y. Castin, “Eur. Phys. J. D **4**, 247”, 1998
- [39] M. R. Andrews, C. G. Townsend, H. J. Miesner, D. S. Durfee, D. M. Kurn and W. Ketterle, “Science **275**, 637”, 1997
- [40] Y. Shin, M. Saba, T. A. Pasquini, W. Ketterle, D. E. Pritchard and A. E. Leanhardt, “arXiv:cond-mat/0306305”, 2003

-
- [41] M. Griener, O. Mandel, T. Esslinger, T. W. Hansch and I. Bloch, “Nature **415**, 39”, 2002
- [42] H. M. Wiseman, “J. Opt. B, **6**, S849”, 2004
- [43] K. V. Kheruntsyan and P. D. Drummond, “Phys. Rev. A **66**, 031602(R)”, 2002
- [44] D. F. Walls & G. J. Milburn, “*Quantum Optics*”, Springer-Verlag, 1995
- [45] D. J. Griffiths, “*Introduction to Quantum Mechanics*”, Prentice Hall, 1995
- [46] T. M. Hanna, “*Some Progress Made*”, ACQAO Project Report, 2004
- [47] Joseph Hope, Private communications, The ANU, 2004